Quasi-Biennial Oscillation Modulation of Global Monsoon Systems and Regional Teleconnections

Vinay Kumar[1#], Shigeo Yoden[2], Matthew H. Hitchman[3], Tetsuya Takemi[4], and Kosuke Ito[4]

[1]Radio and Atmospheric Physics Lab, Rajdhani College, University of Delhi, New Delhi, 110 015, India
[2]Professor Emeritus of Kyoto University, Kyoto, 606-8501, Japan
[3]Department of Atmospheric and Oceanic Sciences, University of Wisconsin–Madison, Madison, WI, 53706, USA
[4]Disaster Prevention Research Institute, Kyoto University, Kyoto, 611-0011, Japan

[#]*Correspondence to*: Vinay Kumar (dabas.vinay@gmail.com)

Abstract. This study investigates the influence of the stratospheric Quasi-biennial oscillation (QBO) on global monsoon systems and their extratropical teleconnections using 42 years (1979–2020) of monthly mean ERA-5 reanalyses data. QBO modulation of precipitation and circulation variables is examined ~~in the context of downward progressing QBO phases,~~ separately for June, July, and August (JJA) and December, January, and February (DJF). It is found that QBO teleconnections act primarily by modulating regional circulations. During JJA, QBO westerly (W) at 50 hPa coincides with an intensified Pacific Walker Circulation (WC), with enhanced rainfall over the Maritime Continent and less over the Western Pacific. In the Northern Hemisphere (NH) subtropics for the same QBO W, the anticyclonic lower tropospheric circulation in the Northwest Pacific is reduced, with rainfall south of Japan shifting eastward. During DJF, QBO teleconnections with the North Atlantic Oscillation (NAO) and the Pacific–North America (PNA) patterns are observed. QBO W at 50 hPa promotes a positive NAO, with an~~hich~~ enhances ~~the anticyclonic circulation associated with the~~ Azores High, a ~~resulting in a stronger~~stronger North Atlantic jet stream, and a westward shift in precipitation toward ~~the east coast of~~ North America. While the ~~As QBO phase progress,~~ QBO W at 70 hPa promotes a positive PNA phase, with a trough over the Gulf of Alaska and ridge over the Eastern Pacific. This promotes northeastward flow into Alaska and above average precipitation, with ~~less~~ reduced precipitation along the west coast of the United States. In each of these examples, the opposite effect is observed during QBO easterly (E) relative to QBO W~~, suggesting the dominance of linearity in QBO modulations~~.

1. Introduction

The global monsoon (GM) is a large-scale circulation system which helps to control the distribution of precipitation in low- and mid-latitudes. It responds to the annual cycle of solar forcing and energy budgets (Bordoni and Schneider, 2008; Biasutti et al., 2018; Geen et al., 2020), and is influenced by continental-scale thermal contrast between land and ocean (e.g., Chang et al. Eds., 2005; Krishnamurti et al., 2013). In the GM system, specific features of the underlying surface, including the land-ocean distribution, topography, and oceanic circulation play key roles in contributing to regional differences observed among monsoon systems (Wang and Ding, 2008; Wang et al., 2017). Based on the timing of the wet season, the summer GM can be classified into two main modes: the boreal summer monsoon (June, July, and August, hereinafter JJA) in the Northern

Hemisphere (NH) subtropics, and the austral summer monsoon (December, January, and February, hereinafter DJF) in the Southern Hemisphere (SH) subtropics (An et al., 2015). During JJA the~~Further, at the regional scale, the summer GM is categorized in six dominant monsoon systems in the world:~~ three primary regional monsoon systems are North African, Asian, and North American, while during DJF they are ~~in NH during JJA, and~~ South African, Australian, and South American ~~in SH during DJF~~. These regional monsoons are not independent but have a dynamical linkage among them via prevailing wind patterns (Meehl, 1987). In the past few decades there has been a series of research publications and review articles ~~on the GM~~ which describe the complexity of the GM system (e.g., Chang et al. Eds. 2005; 2011; 2016; 2020; Yoden et al., 2023). ~~However, the GM is a complex system, and i~~Its variability across different time scales has a profound societal and economic impact on nearly two-thirds of the world's population. Thus, studying variations in the GM system across subseasonal, seasonal, interannual, and decadal timescales is essential for~~to~~ improving~~e~~ knowledge and forecasting skill. Forecasting variations in GM dynamics across different time scales remains challenging~~, due to the highly complex characteristics of teleconnections with various atmospheric circulations~~. Understanding interannual variability of the GM system presents a significant challenge to the scientific community. An improvement in understanding would directly benefit society through an improved ability to forecast regional and seasonal climate anomalies.

On interannual time scales, the GM system is also influenced by the stratospheric quasi-biennial oscillation (QBO) and the El Niño Southern Oscillation (ENSO). The QBO can influence global monsoon structures via mean meridional circulation (MMC) cells by modulating the upper troposphere and lower stratosphere (UTLS) directly, or through the stratosphere via annular modes. ~~–~~ ENSO can influence the GM by modulating the distribution of SSTs and tropospheric circulation. Through modulation of tropical convective centers, both the QBO and ENSO can modulate the Rossby source term (Chapter 8, James 1994), and therefore modify climatological structures associated with stationary Rossby wave trains, including the Pacific-North America pattern (PNA) and North Atlantic Oscillation (NAO).

ENSO is~~,~~ a major driver of global teleconnections (Mooley and Parthasarathy, 1984; Shen and Lau, 1995; Krishnamurthy and Goswamy, 2000; Yu et al., 2021). ~~The impact of ENSO can be confined to a specific monsoon system and may vary with the time scale.~~ Over the Northwest Pacific, ENSO significantly modulates regional atmospheric circulation and associated precipitation patterns (Wang et al., 2024). As a remote teleconnection with the North Atlantic, ENSO induces variability in the NAO, leading to shifts in the jet stream location and strength, modulating weather conditions across Northern Europe and the Eastern United States (Hurrell et al., 2003). In the North Pacific, ENSO anomalies modulate the PNA pattern, where La Nina favors more precipitation in Alaska (Wendler et al. 2017), and El Nino favors more precipitation in California (Jong et al. 2016). Recently, Yu et al. (2021) demonstrated that, at interannual time scales, the Indian summer monsoon exhibits a ~~strong~~significant~~er~~ relationship with ENSO~~, whereas on the decadal time scale, this relationship is weaker~~. Despite extensive studies on the teleconnection between GM dynamics and surface atmospheric circulations, interannual variability of the GM is still unclear, and further research is needed to improve understanding.

~~Vertical coupling with stratospheric phenomena can also influence the GM system.~~ The ~~quasi-biennial oscillation (~~QBO~~)~~ is a regular dynamical feature of the equatorial stratosphere ~~in the layer ~ 10-100 hPa,~~ in which alternating layers of

easterly (E) and westerly (W) winds descend in time, with a range in periodicity ~~–~~ of 24-32 months (Baldwin et al., 2001). The influence of the QBO is not confined to the equatorial~~tropical~~ stratosphere, but can extend down to the surface across the entire globe through two~~three~~ primary pathways, ~~described as~~ the ~~tropospheric~~UTLS pathway and stratospheric~~e~~ pathway~~s~~ (Hitchman et al. 2021). ~~These two pathways can be~~ QBO mean MMC modulate the temperature structure of the tropical and subtropical UTLS in an antiphased sense, where descending QBO W is associated with a warm anomaly in the tropics and simultaneous cold anomalies in the subtropical UTLS of both hemispheres (Hitchman et al. 2021). Modulation of tropical deep convection can alter the planetary wave pattern radiating along the UTLS into the extratropics. Direct modulation of the subtropical westerly jets (STJs) via QBO MMC can involve feedback with synoptic waves, so this part of the UTLS pathway is often studied separately as the "subtropical route". Haynes et al. (2021) classify these pathways into ~~–~~the tropical, subtropical, and polar routes. The "UTLS pathway" refers to QBO modulation of the tropics and subtropics, with effects propagating along the UTLS into the extratropics, altering planetary wave patterns and jets ~~by directly affecting tropical convection, by affecting the interaction between subtropical jets (STJs) and synoptic waves, and via the winter stratosphere (Haynes et al., 2021;~~(Kumar et. al., 2022, 2024) and therefore regional GM circulations. ~~The tropical and subtropical pathways are caused by QBO modulation of the zonal mean temperature structure in the upper troposphere and lower stratosphere (UTLS) by QBO mean meridional circulation (MMC) cells, where descending QBO W is associated with a warm anomaly in the tropics and simultaneous cold anomalies in the subtropical UTLS of both hemispheres (Hitchman et al. 2021).~~

The "stratospheric pathway", or polar route, connects to the surface via the winter stratosphere. The polar route ~~stratospheric pathway~~ involves QBO modulation of planetary Rossby wave propagation by changing the stratospheric QBO MMC and position of the zero-wind line. This pathway ~~is known as~~gives rise to "Holton-Tan effect", or H-T effect (Holton and Tan 1980; 1982), which operates during boreal winter when westerlies exist in the polar stratosphere. ~~–~~, QBO E at 30 hPa favors a disrupted polar vortex, and therefore a weak Northern Annular Mode (NAM) and increased midlatitude surface cold air outbreaks (e.g., Kumar et al., 2022). In the subtropical route, when a QBO MMC pattern arrives at the tropopause, it ~~causes antiphased temperature anomalies in the tropics and subtropics, which~~ alters the meridional temperature gradient, and consequently ~~, hence~~ the distribution of zonal wind~~,~~ by the thermal wind law. The resulting changes in static stability and wind shear in the UTLS can affect deep convection (Giorgetta et al. 1999, Collimore et al. 2003, Nie and Sobel, 2015). The resulting QBO zonal wind anomalies can influence the STJs, which can, in turn, interact with synoptic and ~~and~~ planetary-scale waves~~eddies~~ which originate in the extratropics and dissipate in the subtropics (Garfinkel and Hartmann, 2011; Inoue and Takahashi, 2013; Haynes et al., 2021). In the tropical route, dynamical and thermodynamic modulation of the tropical UTLS by the QBO MMC is directly linked to the surface ~~region~~ through modulation of deep convection and its organization (Gray et al., 1992a, 1992b; Collimore et al., 1998, 2003; Kumar et al., 2014; Lee et al. 2019; Hitchman et al., 2021; Haynes et al., 2021). QBO modulation of deep convective centers can modulate the planetary wave trains which emanate from them, with poleward energy dispersion along the UTLS. This can, in turn, modulate regional circulation features in the extratropics, including the ~~North Atlantic Oscillation (~~NAO~~)~~ and ~~Pacific North America (~~PNA~~)~~ patterns. Information about QBO phase can be used to improve ENSO prediction (Rodrigo et al., 2025).

QBO modulation of deep convection in the tropical route may play a substantial role in tropical rainfall and global circulation, potentially influencing forecasts of weather around the globe (Collimore et al., 2003). Gray et al. (2018) observed increased precipitation in the tropical Western Pacific when there is QBO W at 70 hPa, particularly during boreal summer. They also noted that the band of precipitation across the Pacific, associated with the intertropical convergence zone (ITCZ), shifts southward. In the subtropical route, the QBO may directly influence rainfall in the subtropics. For example, when QBO E occurs at 70 hPa, the East Asian STJs weakens and shifts poleward, weakening the East Asian winter monsoon (Ma et al., 2021).

The effects of the QBO on rainfall in different parts of the globe, particularly within the tropical and subtropical regions, have been examined in some previous observational studies (Seo et al., 2013; Gray et al., 2018; Ma et al., 2021). In addition, several numerical modeling studies have been conducted to explore modulation of rainfall patterns by the QBO (Goswami, 1998; Giorgetta et al., 1999; Brönnimann et al., 2016). However, some contradictions have been observed among the numerical model studies. In a general circulation model (GCM) experiment, Giorgetta et al. (1999) found that the boreal summer monsoon ~~JJA~~ is significantly influenced by the QBO, with the less precipitation over the Western Pacific during QBO W but more over the Indian Ocean. On the other hand, Brönnimann et al. (2016) did not find significant QBO effects on the Indian monsoon in either observations or coupled ocean–atmosphere–chemistry climate model simulations.

Recently Yoden et al. (2023) reported on new observational aspects of QBO modulation in~~of~~ the GM system, highlighting modulation of low-pressure cyclonic perturbations over the NH Western Pacific during JJA and Eastern Pacific during DJF. However, this study does not provide an in-depth view of the QBO association with the GM system from both a phenomenological and mechanical perspective. In a very recent study, Kumar et al. (2024) demonstrated teleconnections between the QBO and regional surface climate in Eurasia and North America during boreal winter. They proposed a ~~new~~ teleconnection pathway via the UTLS region to the high-latitude surface, independent of the H-T mechanism. Both studies suggest that the role of the QBO in modulating surface weather regimes from the equatorial regions to the polar regions cannot be ignored. Therefore, further systematic work is needed to diagnose the QBO teleconnection pathways, which vary on a seasonal and regional basis and by phase of the QBO.

QBO teleconnections with the tropospheric surface via the different routes discussed above display pronounced zonally asymmetric feature and sensitivity to its vertical phase (Collimore et al. 1998; 2003; Gray et al. 2018; García-Franco et al.2023; Kumar et al. 2024). Collimore et al. (1998, 2003) observed that the QBO primarily modulates convective activity over tropical deep convection, using the 50–70 hPa zonal-mean wind shear as an index. Gray et al. (2018) noted that, during JJA, precipitation over the tropical Western Pacific exhibits maximum sensitivity to QBO winds at 70 hPa. On the other hand, Zhou et al. (2024) observed that precipitation over the Yangtze–Huaihe River Basin (YHRB) during JJA is sensitive to QBO winds at 50 hPa.

During DJF, the 50 hPa QBO index has been extensively used to assess changes in the NAM via H-T mechanics, in order to evaluate its modulation of mid-latitude surface dynamics. Recently Kumar et al. (2024) used the 70 hPa QBO index and described a teleconnection pathway via the UTLS to the Eurasian and North American surface that is independent of the

H–T mechanism. The present study uses 50 hPa and 70 hPa QBO indices, since these levels exhibit the most consistent phase relationship with QBO phase in the UTLS, and are compatible with most previous studies. The QBO signal in tropical precipitation exhibits significant zonal asymmetries at a regional scale (Gray et al. 2018; García-Franco et al. 2023; Yoden et al. 2023). Garcia-Franco et al. 2023 found much larger QBO differences in precipitation over the oceans. The present study is intended to provide a first-step global perspective by identifying regions where the QBO signal is most evident in the zonally-asymmetric GM circulation systems.

The phase of ~~Also, the~~ ENSO ~~events~~ can enhance or diminish the ~~directly~~ influence the QBO ~~MMC, tropical, subtropical and polar routes~~ (Kumar et al., 2022). The new teleconnection pathway observed by Kumar et al. (2024) was found to exist only during the neutral phase of ENSO (neither El Niño nor~~or~~ La Niña). Yoden et al. (2023) ~~also~~ excluded extreme El Niño and La Niña events to avoid contamination by~~from~~ them. I~~Therefore, i~~n this study~~,~~ we will also focus on ~~the~~ neutral ENSO ~~ESNO~~ times in order~~period~~ to ~~extract~~ highlight ~~the~~ QBO effects on GM system and regional circulation and precipitation patterns~~, focusing on regions~~ from tropical to extratropical latitudes (60°S-60°N) ~~where monsoon circulations have a strong influence on precipitation and wind patterns~~. Potential routes by which the QBO connects with the GM system will be investigated, focussing on changes associated with specific QBO phase pairs~~s~~. Separate analyses are presented for ~~both~~ the JJA and DJF seasons. ~~This study examines not only precipitation and its proxy data but also circulation fields. The sensitivity of QBO surface teleconnection modulation to the downward propagating QBO phase is investigated by systematically varying the altitude of QBO index to search for prominent remote influences of the QBO on the GM system.~~

2. Data and methodology

2.1 Data

Monthly mean ERA-5 reanalysis data for the 42-year period 1979 - 2020 (satellite era) are used to analyze ~~the various meteorological variables such as~~ zonal and meridional wind (U, V), vertical wind (W), divergence of horizontal wind, specific humidity (q), ~~and~~ mean sea level pressure (MSLP), and geopotential height (GPH). ERA-5 offers several improvements over ~~its preceding~~ ERA-Interim ~~version (Hersbach et al., 2020)~~, having ~~as it is~~ benefitted from a decade of development~~s~~ in core dynamics~~,~~ and model physics (Hersbach et al., 2020). A~~The a~~ssimilation of a much larger number of reprocessed datasets has improved ERA-5 reanalysis products ~~which is considerable in the troposphere~~. In this study, a double prime superscript for a given meteorological variable, $\boldsymbol{X''}$, represents de-seasonalized anomalies, or ~~, its~~ deviation from the climatological seasonal mean ~~annual cycle~~ in the 42-years data set~~the 42-years climatological mean for that month~~. . Vertical wind shear of the zonal mean zonal wind (dU/dz) is calculated using centered finite differencing.

Monthly mean values of o~~O~~utgoing longwave radiation (OLR) ~~monthly data are taken~~were obtained from the National Oceanic and Atmospheric Administration (NOAA) (Gruber and Krueger 1984). To study the monsoon patterns, precipitation (P) data we~~a~~re ~~used~~ obtained from the Global Precipitation Climatology Project (GPCP) version 2.3, which~~. This merged data set~~ incorporates precipitation estimates from surface rain gauge stations, low-orbit satellite microwave data, and

geostationary satellite infrared data, on a 2.5° × 2.5° (latitude × longitude) global grid (Adler et al., 2003; 2018). This dataset provides an overview ~~a definitive description~~ of global monsoon rainfall patterns over both land and ocean.

SST data ~~were~~ are obtained from the Hadley Centre Global Sea Ice and Sea Surface Temperature (HadISST) v1.1 (Rayner et al., 2003) and are used to calculate the monthly Niño 3.4 index for identifying extreme ENSO events. These events are defined using de-seasonalized data over a 42-year period in the Niño 3.4 region (5°N–5°S, 120°W–170°W). Any month is considered to be an extreme El Niño or La Niña period whenever the Niño 3.4 index exceeds the threshold values ±1.0 K (+: El Niño; –: La Niña). ~~;~~ W~~w~~e obtained 395 neutral, 57 El Niño, and 52 La Niña months. This study focuses on the 395 neutral-to-moderate months only, and all the analysis is conducted at 2.5° × 2.5° resolution, spanning 60°S to 60°N.

2.2 Methodology

A QBO state is defined in a two-dimensional phase space using the first two principal components (*PC1* and *PC2*) of the de-seasonalized zonal mean zonal wind variations in the equatorial lower stratosphere between 10 hPa to 70 hPa (Wallace et al., 1993). Figure S1 in supportive information (hereinafter SI) shows the vertical structure of the first two leading EOFs, along with scatter plots in the *PC1* and *PC2* phase space for all four seasons: DJF, March, April, and May (MAM), JJA, and September, October, and November (SON). The QBO state is represented by the phase angle $\boldsymbol{\theta = tan^{-1}\left(\frac{PC2'}{PC1'}\right)}$, where $PC1'$ and $PC2'$ are the principal components with respect to the centroid of all data points (black + marker in Fig. S1). See Kumar et al. (2022, 2024) and Yoden et al. (2023) for a detailed description of the methodology used in employing EOF analysis to define QBO phase. In this study we divide QBO phase into the following eight 45° angular bins: phase 1 (0 – 45°), phase 2 (45 – 90°), phase 3 (90 – 135°), phase 4 (135 – 180°), phase 5 (180 – 225°), phase 6 (225 – 270°), phase 7 (270 – 315°), and phase 8 (315 – 360°), hereinafter designated P1 to P8 (Hitchman et al., 2021; Yoden et al., 2023).

Figure 1 shows vertical profiles of the composite means of de-seasonalized zonal mean zonal wind at the equator, for each of the eight phases separately, during JJA (a-d) and DJF (e-h). Each subplot contains two profiles corresponding to opposite QBO phases at the central angle $\boldsymbol{\theta_c}$ (i.e., $\boldsymbol{\theta_c}$, and $\boldsymbol{\theta_c + 180°}$), shown in red for P1 to P4 and blue for P5 to P8. The composite difference between the opposite phases is shown as a black dashed line (Fig. 1). An open circle on the right y-axis indicates that the composite difference for a given level is statistically significant (90%), using a two-sided Student's *t*-test with two independent samples in each phase. Successive downward phase propagation of QBO W (QBO E) phase can be seen from P1 to P4 (P5 to P8) between 20 hPa and 70 hPa. Most of the major features of QBO propagation are similar in the two seasons for each phase pair (Fig. 1).

However, w~~W~~hen QBO winds maximize at 70 hPa with the opposite phase at 20 hPa, the profile of P1-P5 is different above ~~0.~~3 hPa for JJA (Fig. 1a) and DJF (Fig. 1e). Further, it is also noteworthy that~~and~~ the magnitude of P1-P5 in the lowest stratosphere is diminished during DJF. At 70 hPa, the whiskers are clearly separated in the JJA profile (Fig. 1a), but overlap in the DJF profile (Fig. 1e). Kumar et al. (2013) showed that the tropopause height is at a higher altitude (~ 90 hPa) during DJF compared to JJA (~ 110 hPa) (see also Reid and Gage 1985). ~~, suggesting that the higher tropopause during DJF may be inhibiting deeper penetration of the QBO signal to the troposphere.~~ Note that DJF is a dynamically active season in the NH

(and during SON in the SH), with westerly winds permitting upward propagation of planetary waves into the stratosphere and the possibility of the H-T mechanism. Also~~, the~~, deep convection penetrates higher over Indonesia during DJF, so that~~the~~ cloud tops would ~~"poke up higher"~~extend higher into QBO thermal anomalies associated with the MMC, which can modulate ~~upper tropospheric~~ static stability~~instability in deep convection~~. Furthermore, the pattern of convection is more symmetric about the equator during DJF, subject to the tropical QBO UTLS anomaly. From ~~this mechanism~~these considerations, one might expect ~~the~~ significant QBO effects during DJF ~~for the tropical route~~in the tropics. ~~On another hand, during JJA, a lack of stratospheric westerlies implies that the teleconnection likely occurs along the subtropical UTLS. So, seasonality is an important factor in understanding QBO dynamical teleconnections.~~ During JJA convection shifts northeastward to Southeast Asia from the Maritime Continent and northeastward from Brazil to the Gulf of Panama, both in the subtropics. Thus, during JJA convection in the subtropics is subject to the opposite sign of QBO UTLS thermal anomaly compared to the tropics. Keeping this antiphased zonal mean pattern in mind will be helpful in diagnosing QBO influences during JJA compared to DJF.

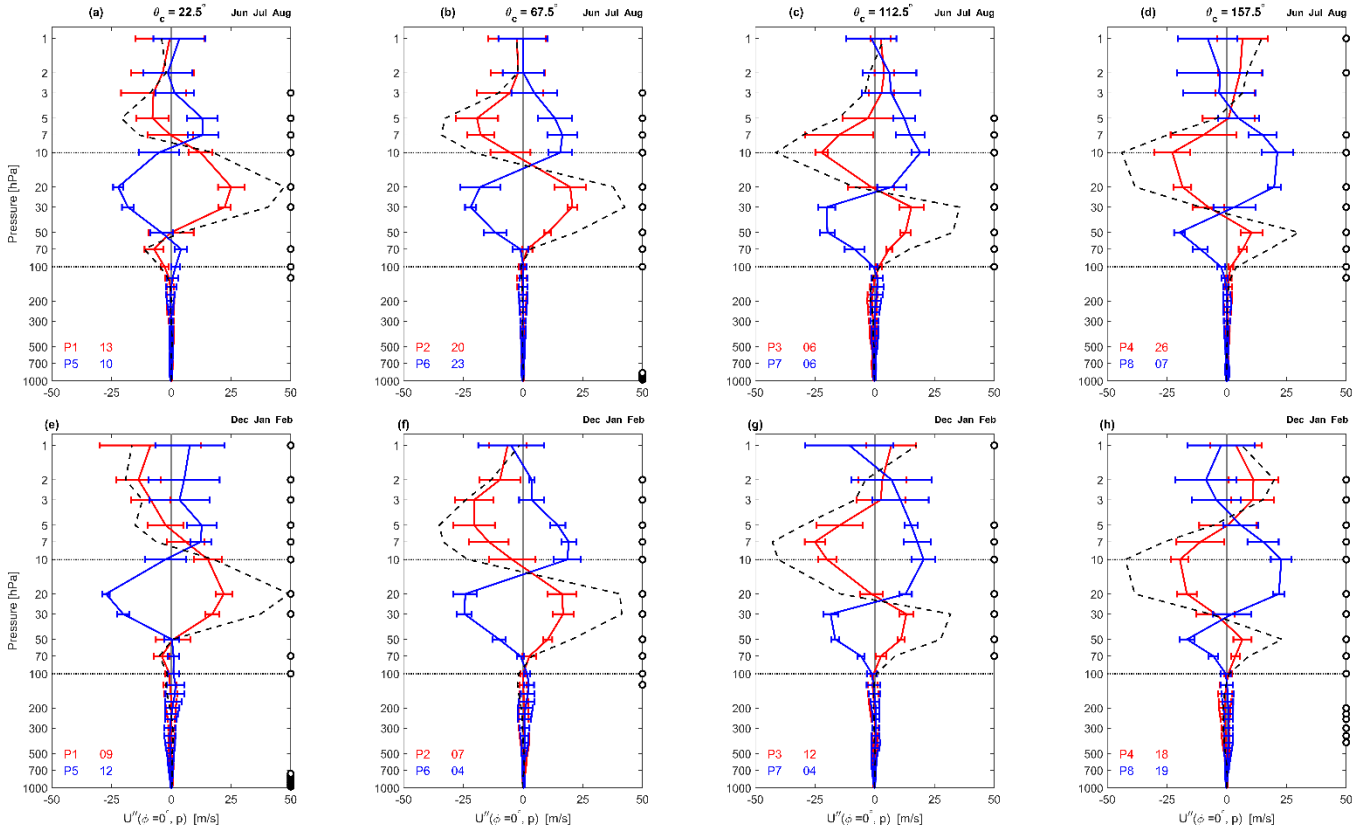

Figure 1. Average vertical profiles of zonal mean zonal wind **U′′** anomalies for each of the eight phases P1 to P4 (red) and P5 to P8 (blue), along with composite differences between these QBO opposite phases (black dashed line) for JJA (a-d) and DJF (e-h). The whiskers denote ± one standard deviation for each composite phase, and an open circle is plotted on the right y-axis if the composite difference at that level exceeds 90% statistical significance. The total number of samples for each phase is written at the bottom left corner in each panel.

Based on our previous survey of modulations of the GM system by QBO phase (Yoden et al., 2023), this study will focus on the phases when QBO anomalies arrive in the UTLS regions, separately for JJA and DJF~~,~~. R~~with r~~esults are presented for the composite differences P4 – P8 (QBO W – ~~QBO~~ E at 50 hPa)~~, as well as for~~ and P5 – P1 (QBO W – ~~QBO~~ E at 70 hPa). For an easy understanding of the QBO signature in the GM system, it is essential to grasp the fundamental dynamics of the GM system; therefore, we will first discuss its climatology briefly in the next section.

3. Climatological cycle of the GM

Figure 2 provides an overview of the 42-year zonal mean and non-zonal climatology of the GM system in precipitation and~~(P), together with the~~ winds ~~patterns (U, V)~~ at 950 hPa~~, , and~~ showing~~presents~~ the annual mean, JJA mean~~boreal summer monsoon JJA,~~ ~~and austral summer monsoon~~ DJF mean, and JJA-DJF mean ~~structures~~ patterns separately~~,~~. ~~This climatology is created~~ using only neutral ENSO months. ~~The 1st column represents the zonal mean structure of [U] (solid line) and [V] (dashed line). The 2nd column shows zonal mean precipitation [P], while the 3rd column shows a longitude-latitude section of precipitation (P) along with arrows representing (U, V) wind patterns. From top to bottom, rows show the mean states for all year, JJA, DJF, and the composite difference JJA – DJF. Note that a positive value (golden color) in the composite difference panel denotes the region of heavy precipitation during JJA in comparison to DJF, and a negative value (green color) denotes the region of heavy precipitation during DJF compared with JJA.~~ The composite difference panel provides a concise overview of seasonal variations in global monsoon precipitation, a phenomenon extensively examined in numerous previous studies (Wang and Ding, 2008; Bordoni and Schneider, 2008; Biasutti et al., 2018; Geen et al., 2020). This figure is an updated version of Fig. 3 of Yoden et al. (2023), showing a wider latitudinal domain, from 60°S to 60°N, and including wind patterns in the boundary layer at 950 hPa.

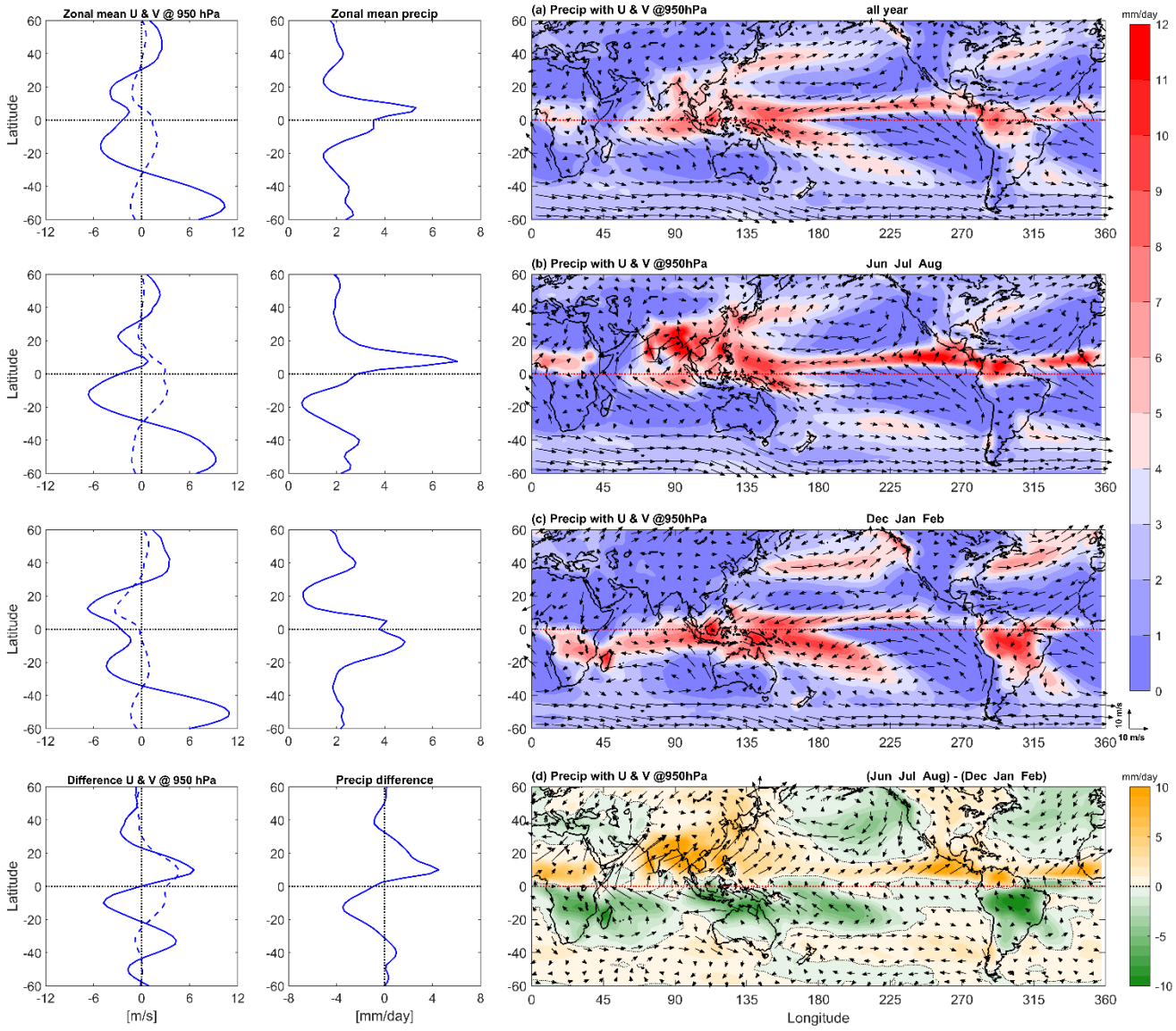

Figure 2. ERA-5 climatology (1979-2020) of precipitation (P) and horizontal winds (U, V) at 950 hPa, using only neutral ENSO months. The 1st and 2nd columns show latitudinal profiles of zonal mean zonal [U] (solid line) and meridional [V] (dashed line) winds, and zonal mean precipitation [P], respectively. The 3rd column shows charts of precipitation P (color bar) along 950 hPa wind vectors. From top to bottom, rows show results for the climatological a) annual mean, b) boreal summer monsoon (JJA), c) austral summer monsoon (DJF), and d) the composite difference JJA – DJF, respectively. In d), a positive value (golden color) denotes enhanced precipitation during JJA relative to DJF, and a negative value (green color) denotes enhanced precipitation during DJF relative to JJA.

Seasonal variations between JJA and DJF can be clearly seen in the zonal mean and geographically-varying structure of precipitation and horizontal wind vectors. Note there is very little shift in the ITCZ in the Pacific, but the latitude of the zonal mean maximum shifts from ~~a seasonal shift of the ITCZ from~~ ~ 7°N in ~~the annual and~~ JJA ~~averages~~ to ~10°S in DJF

(Fig. 2, 2nd column). Vigorous convection over Brazil and the South Pacific Convergence zone contribute strongly to the zonal mean in DJF. In the composite difference JJA – DJF panel, [U] and [P] show roughly anti-symmetric profiles with respect to the equator, whereas [V] is roughly symmetric, describing the annual cycle responses with a half-year time difference between the two hemispheres and the asymmetry of the Hadley circulation at the solstices.

The composite difference chart of precipitation and 950 hPa winds (Fig. 2d) highlights the prominent regional monsoon systems over the globe. During boreal summer monsoon JJA in the NH, heavy precipitation is associated with the North African, Asian, and North American monsoons (Fig.2b, golden shading in Fig. 2d). These monsoon precipitation patterns are associated with dominant large-scale wind circulations. The northward flow in the boundary layer associated with the Hadley cell occurs in preferred longitude bands, including prominent cross-equatorial winds over Indonesia, over the western Indian Ocean (which feeds the Somali Jet), over the Eastern Pacific, and Eastern Atlantic Oceans, each of which brings moisture toward heavy precipitation regions along the ITCZ (Fig. 2-b, d). The North Atlantic and North Pacific are dominated by large surface anticyclones, which generate less precipitation but transport moisture clockwise from the subtropics, creating a band of higher precipitation to the northwest of the anticyclones (Fig. 2b).

The monsoon circulation during ~~austral summer~~ DJF also exhibits a longitudinal preference for cross-equatorial flow in the boundary layer toward the summer hemisphere, notably in the Western Pacific and Western Atlantic, which feed into regional precipitation maxima over South Africa, the Amazon, and a band stretching from the South Pacific Convergence Zone (SPCZ) in the Southwest Pacific across the Indian Ocean (Fig. 2c). These regional precipitation maxima are highlighted by green shading in the JJA – DJF difference plot (Fig. 2d). As in the NH during JJA, large anticyclones are prominent over the mid-latitude Indian, Pacific, and Atlantic Oceans of the SH during DJF, which help feed moisture poleward on their west edges, creating thin midlatitude precipitation maxima poleward of the anticyclones. Seasonal characteristics of other meteorological variables are shown in Figure S2 ~~of SI in (a-g) panels~~ as JJA – DJF ~~composite~~ differences for ~~(b)~~ OLR, ~~(c) upper tropospheric~~300 hPa specific humidity~~, q, at 300 hPa~~, ~~(d)~~ SST, ~~(e)~~ MSLP and 950 hPa winds~~with (U, V) at 950hPa~~, ~~(f) horizontal wind~~950 hPa divergence ~~at 950 hPa~~, and ~~(g)~~500 hPa ~~mid tropospheric~~ vertical velocity ~~wind at 500 hPa~~. ~~Seasonal variations in these meteorological variables exhibit systematic association with the composite difference of precipitation, P. Variations in OLR are somewhat smoother than those in P, having larger scale patterns compared to the spatial scales of variation of the precipitation field.~~ Deep convective features appear as opposite-sign peaks of OLR difference across all six regional monsoon systems (Fig. S2b). ~~Seasonal changes in 300 hPa q and SST are nearly anti-symmetric about the equator. Seasonal differences in MSLP are largest over eastern Eurasia (negative in JJA – DJF) and over the Pacific Ocean (positive in JJA – DJF) in the NH mid-latitudes. Horizontal divergence at 950 hPa shows air mass convergence into regions of higher precipitation. Small scale features tend to dominate divergence fields, partly due to the effects of topography. The pattern of vertical wind at 500 hPa closely resemble the precipitation patterns, with stronger upward motion occurring over areas of higher precipitation.~~ A more detailed description on the climatology and seasonality of all these meteorological variables can be found in Yoden et al. (2023).

4. Zonal mean seasonal structure of QBO

Deseaonalized anomalies of zonal mean zonal wind and temperature between 60°S to 60°N, binned using QBO W-E paired phase indices at 50 hPa (P4 – P8)~~-~~, are used~~In order~~ to investigate the seasonal dependency of QBO dynamical teleconnections ~~, the mean canonical form of zonal mean u-wind, and temperature is constructed between 60°S to 60°N in monthly de-seasonalized anomalies,~~ separately for the boreal and austral monsoon summer seasons (Fig. 3). ~~Figure 3 presents meridional sections of the composite canonical form of U″ and T″ for phase P4 (hereinafter QBO W 50 hPa) and phase P8 (hereinafter QBO E 50 hPa), along with composite differences P4 – P8 (hereinafter QBO W – E 50 hPa) for both JJA and DJF.~~ The antiphased pattern of vertical motion between the tropics and subtropics associated with the MMC is manifested in the UTLS temperature anomalies, such that QBO W causes a tropical warm anomaly and subtropical cold anomalies (Fig. 3c, d). This is more evident during JJA in the subtropics (Fig. 3c), but more evident during DJF in the tropical troposphere (Fig. 3d). From the thermal wind law, integrating upward through the meridional temperature gradients associated with these anomalies yields horseshoe-shaped structures in the QBO W-E zonal wind anomalies (Figs. 3a, b).

During JJA this arch-like structure is absent in the NH subtropics (Fig. 3a). This is the location of the strong upper tropospheric easterlies associated with the equatorward side of the Southeast Asian monsoon during JJA (Krishnamurti 1971). This shows that the Tibetan High and its associated easterly jet may not significantly affected by the QBO. However, note the cold anomaly in the UTLS near 20°N, which can act to reduce static stability above the deep convective center located over Southeast Asia (Fig. 2b) during QBO W at 50 hPa. Note that the corresponding cold anomaly in the SH, acts to shift the winter subtropical jet poleward during QBO W (Fig. 3a).~~During the boreal summer monsoon JJA, the U″ composite difference does not reflect any statistically significant patterns in the troposphere on the NH side (Fig. 3c3a). However, on the SH or winter side, a noticeable pattern of QBO wind anomaly at 50 hPa over the equator extends poleward and downward in an arch shape into the subtropical troposphere, with penetration down to the surface. This arch is accompanied by a vertical anomaly strip of the opposite sign in the mid-latitudes, extending from the surface to the lower stratosphere (50 hPa). Along the UTLS, this dipole favors an equatorward shift of the zonal mean STJs during QBO W at 50 hPa.~~

~~**The checkerboard patterns in T″ anomalies (Figs. 3c, d3g, h, j, k) are consistent with the zonal wind anomaly patterns (Figs.Fig.s 3a, b, c, d) through the thermal wind relationship. This QBO temperature anomaly pattern is caused by the descending QBO MMC, which are more symmetric about the equator during the equinoxes and more asymmetric during the solstices (Hitchman et al., 2021). Stronger temperature anomaly patterns are seen in the winter subtropics (Figs. 3c, d3g, h, j, k). The subtropical QBO temperature anomalies in the lower stratosphere extend poleward and downward along the tropopause, especially on the winter side (SH during JJA and NH during DJF in Figs. 3g, h, j, k). This structure underlies the "horseshoe pattern" in zonal wind anomaly. The large QBO MMC anomalies which extend into the midlatitude stratosphere, causing the temperature anomalies (Fig. 3l3d), are consistent with the patterns of zonal wind response (Figs., 3 fb) in the extratropical winter stratosphere., in the H-T mechanism and stratospheric route discussed by previous authors.~~**

During DJF there is a cold anomaly in the tropical troposphere for QBO W at 50 hPa (Fig. 3d). From the thermal wind law, this implies enhanced, equatorward-displaced subtropical jets near 20°, as are seen in both hemispheres (Fig. 3b). The MMC near 30 hPa is greatly amplified, extending well into the winter hemisphere, causing a large warm anomaly near 40°N (Fig. 3d). Previous studies have shown a stronger extension of QBO MMC into the winter hemisphere (Randel et al., 1999; Kinnersley, 1999; Pena-Ortiz et al., 2008; Hitchman et al., 2021; and Kumar et al. 2022). This implies a weakening of stratospheric westerlies near 30°N during QBO W, as seen in Fig. 3b. The warm anomaly near 40°N is downwelling companion to the upwelling over the equator which underlies QBO E, also implies a strengthening of the polar night jet near 60°N during QBO W, as seen in Fig. 3b. This is a visual representation of the Holton-Tan effect, where QBO W is correlated with a stronger polar night jet.

~~, on the NH or winter side, a noticeable pattern of QBO wind anomaly at 50 hPa over the equator extends poleward and downward in a horseshoe shape into the subtropical regions of both hemispheres, however, the significant patterns on the NH or winter side are limited into UTLS region only (Fig. 3b). On winter side, the QBO wind anomaly of opposite sign at 10 hPa extends poleward and downward into the midlatitude troposphere but significant patterns occur in the upper tropospheric region only (upto 500 hPa). Likewise, JJA on winter side (SH), along the UTLS, this dipole favors an equatorward shift of the zonal mean STJs for QBO W at 50 hPa during DJF on winter side (NH). Tthe significant tropospheric temperature anomalies in the tropics (20°S-20°N) are consistent with a route along the subtropical troposphere (Fig. 3l3d). The QBO MMC in the UTLS simultaneously create antiphased temperature anomalies in the both tropics and subtropics. This implies that the QBO can affect the extratropics along the UTLS by either altering deep convection in the tropics directly, or modulating the temperature and zonal wind near the STJs (Fig. 3b, d). Since any "pure tropical forcing" would have to propagate through the subtropics to get to higher latitudes, the tropical-subtropical route is perhaps best thought of as one route along the subtropical UTLS. QBO anomalies in the tropical UTLS are directly linked with the surface region through modulation of deep convection, especially during DJF (Fig. 3l3d).~~ QBO W at 50 hPa implies a warm anomaly near the tropical tropopause, which lowers the tropopause and stabilizes the upper troposphere, thereby reducing deep convection over Indonesia during NH winter (Collimore et al., 2003), ~~and~~ weakening the Walker Circulation (WC) (Yasunari 1990; Huang et al., 2012; Hu et al., 2012; García-Francoet al., 2022), and causing a warm anomaly throughout the troposphere over Indonesia (Muhsin et al., 2018). The opposite effect for QBO E, with a cold anomaly in the tropical UTLS, warm anomalies in the subtropical UTLS in both the NH and SH, and enhanced convection over Indonesia during DJF. There is also significant modulation of the STJs and polar night jet by QBO MMC. These results suggest that both the stratospheric and UTLS routes for QBO teleconnections operate simultaneously, in addition to the Holton-Tan mechanism during DJF~~, and confirm previous studies showing an equatorially asymmetric, stronger extension of QBO MMC into the winter hemisphere (Randel et al., 1999; Kinnersley, 1999; Pena-Ortiz et al., 2008; Hitchman et al., 2021; and Kumar et al. 2022)~~.

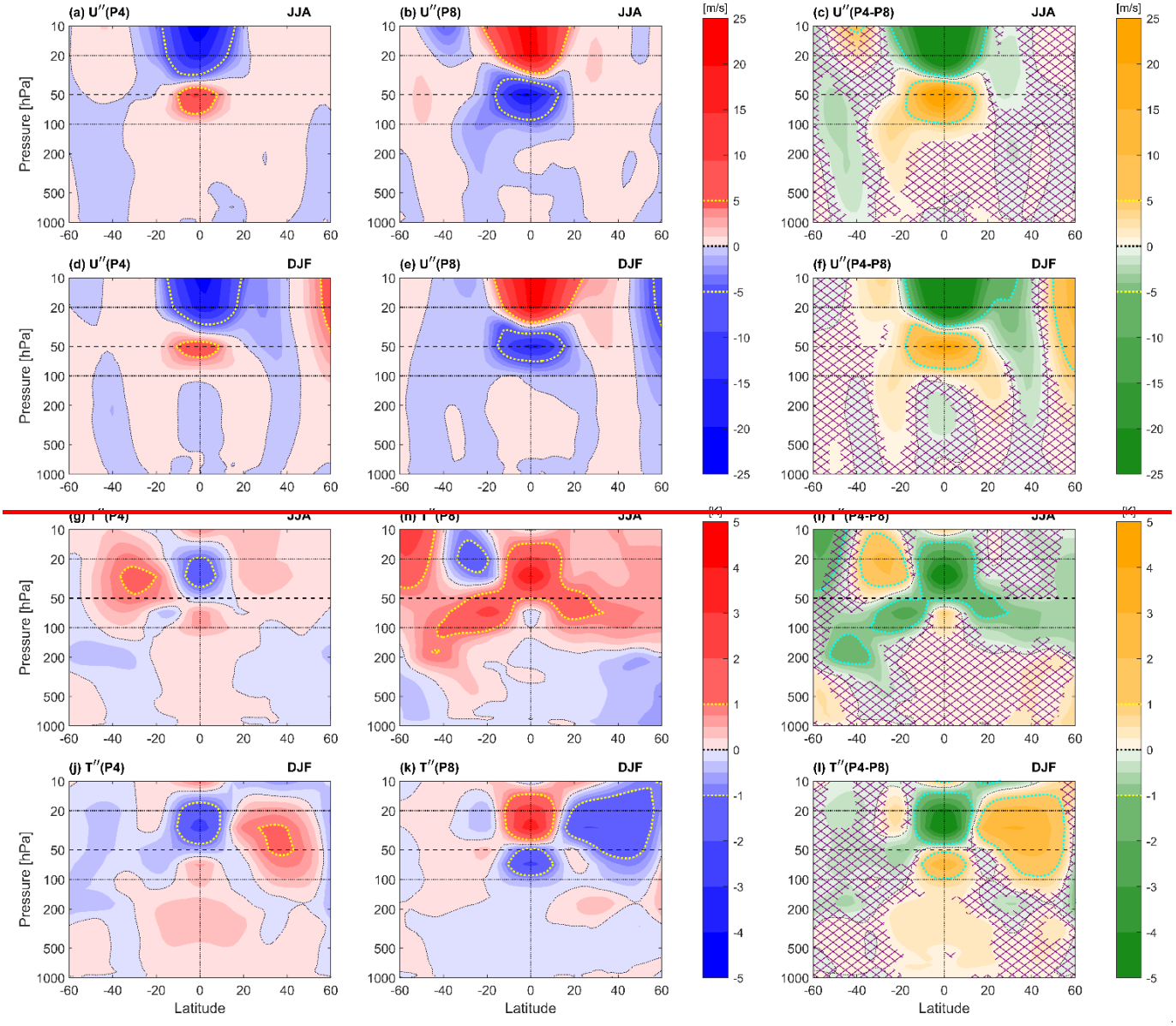
(a) U′′(P4)
JJA
(b) U′′(P8)
JJA
(c) U′′(P4-P8)
JJA
[m/s]
(d) U′′(P4)
DJF
(e) U′′(P8)
DJF
(f) U′′(P4-P8)
DJF
(g) T′′(P4)
JJA
(h) T′′(P8)
JJA
(i) T′′(P4-P8)
JJA
[K]
(j) T′′(P4)
DJF
(k) T′′(P8)
DJF
(l) T′′(P4-P8)
DJF
Pressure [hPa]
Latitude

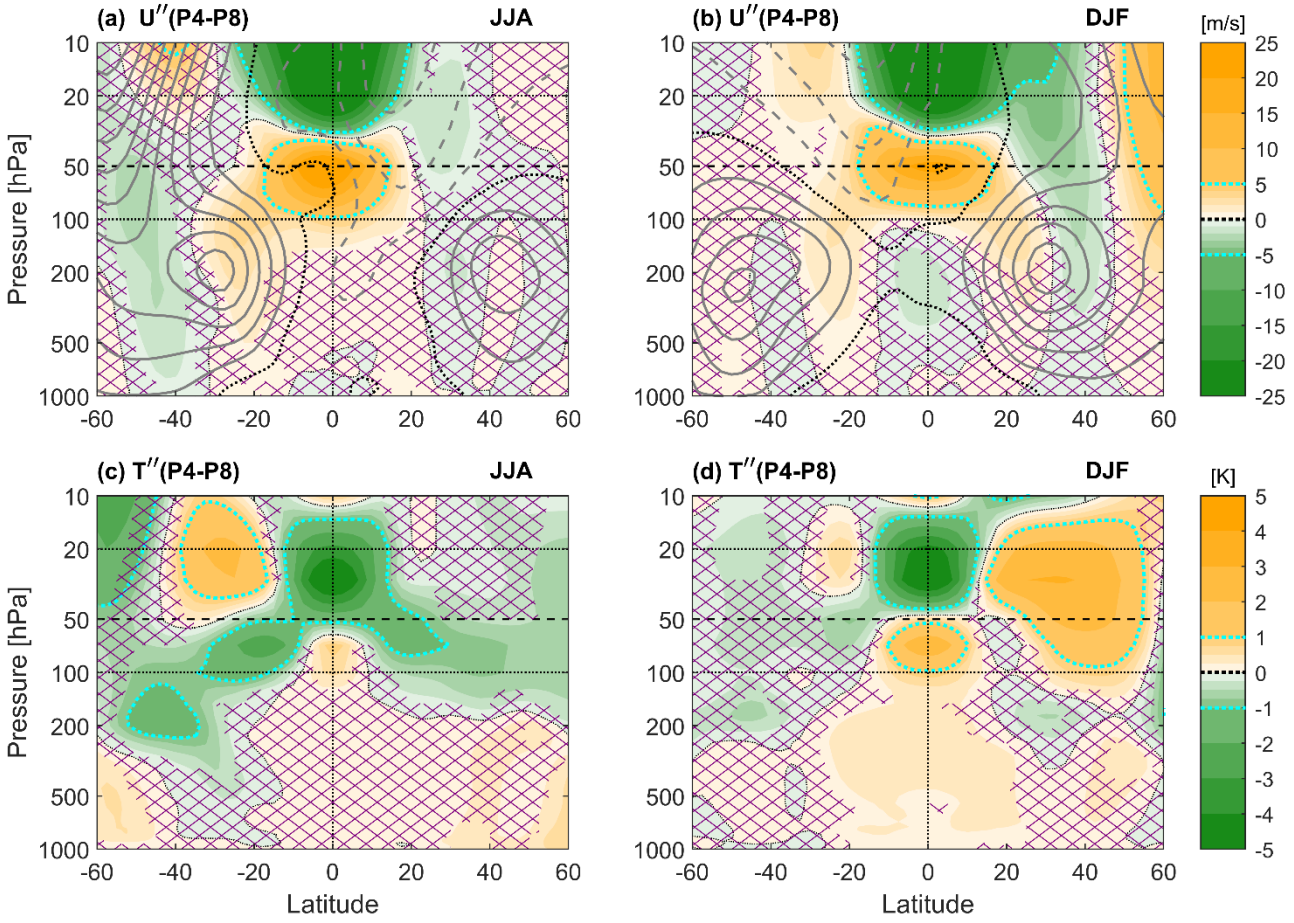

Figure 3. Meridional sections of the composite difference in U" and T" anomalies for opposing QBO phase pairs, QBO W – E at 50 hPa (P4 –P8), during DJF and JJA. Top, a–b) U″ wind anomalies. Bottom, c–d) T″ anomalies. From left to right, columns represent JJA, and DJF. ~~From left to right, columns show anomalies for P4 (QBO W at 50 hPa) and P8 (QBO E at 50 hPa) in blue and red shading (color bar) and P4 – P8 (QBO W – E at 50 hPa) in yellow and green shading (color bar). From top to bottom, rows represent U" wind anomalies for JJA (a–c), U" wind anomalies for DJF (d–f), T" anomalies for JJA (g–j), and T" anomalies for DJF (j–l), respectively~~. The violet cross hatching indicates regions of statistical significance less than 90%. The ~~yellow and~~ cyan dotted line~~s~~ separate regions of fine and coarse contour ~~intervals in the composite and composite differences, respectively~~. Horizontal ~~dashed~~ lines indicate the 20 hPa (dotted), 50 hPa (dashed), and 100 hPa (dotted) levels. The climatological cycle of the U-wind for the period 1970–2020 is also shown as gray contour lines over the U″ wind anomaly panels for the respective seasons. The solid (dashed) contour lines represent the positive (negative) value, and the black dotted line is the position of the zero -wind line.

Figure 4 shows the same seasonal meridional structure of U″ and T″ composite~~s~~ differences as in Fig. 3 but for QBO W – E at 70hPa (P5 – P1) ~~phase P5 (hereinafter QBO W at 70h Pa) and P1 (hereinafter QBO W at 70 hPa)~~. ~~Keying on the 70 hPa level generates a 9 element tic tac toe pattern in the temperature field for both JJA and DJF (Figs. 4c, d4i, l) which is somewhat more coherent than keying on 50 hPa (Figs. 3c, d3i, l).~~ During both JJA and DJF one may see a fundamental~~the~~ tri-pole pattern in temperature anomalies along the subtropical UTLS ~~(Fig.s 4g, h, j, k)~~, with the subtropics antiphased with the

tropics (Fig. 4c, d). The anomalies can extend deep into the troposphere, with considerable differences between the two seasons. During JJA this somewhat complex temperature anomaly pattern is associated with an equatorward shift in the subtropical jet in both hemispheres (Fig. 4a), while during DJF it is associated with a poleward shift in both hemispheres (Fig. 4b). ~~This, in turn, creates QBO zonal wind anomalies which also extend into the troposphere in a tri-pole meridional pattern, again with the tropical tropospheric zonal mean zonal wind anomaly being opposite in sign to those in the subtropics (Figs. 4c, d4a f). This subsequently modifies the strength and position of the subtropical jets STJs.~~ Note that moderate QBO anomalies in temperature and zonal wind are found throughout the troposphere, which can affect surface weather.

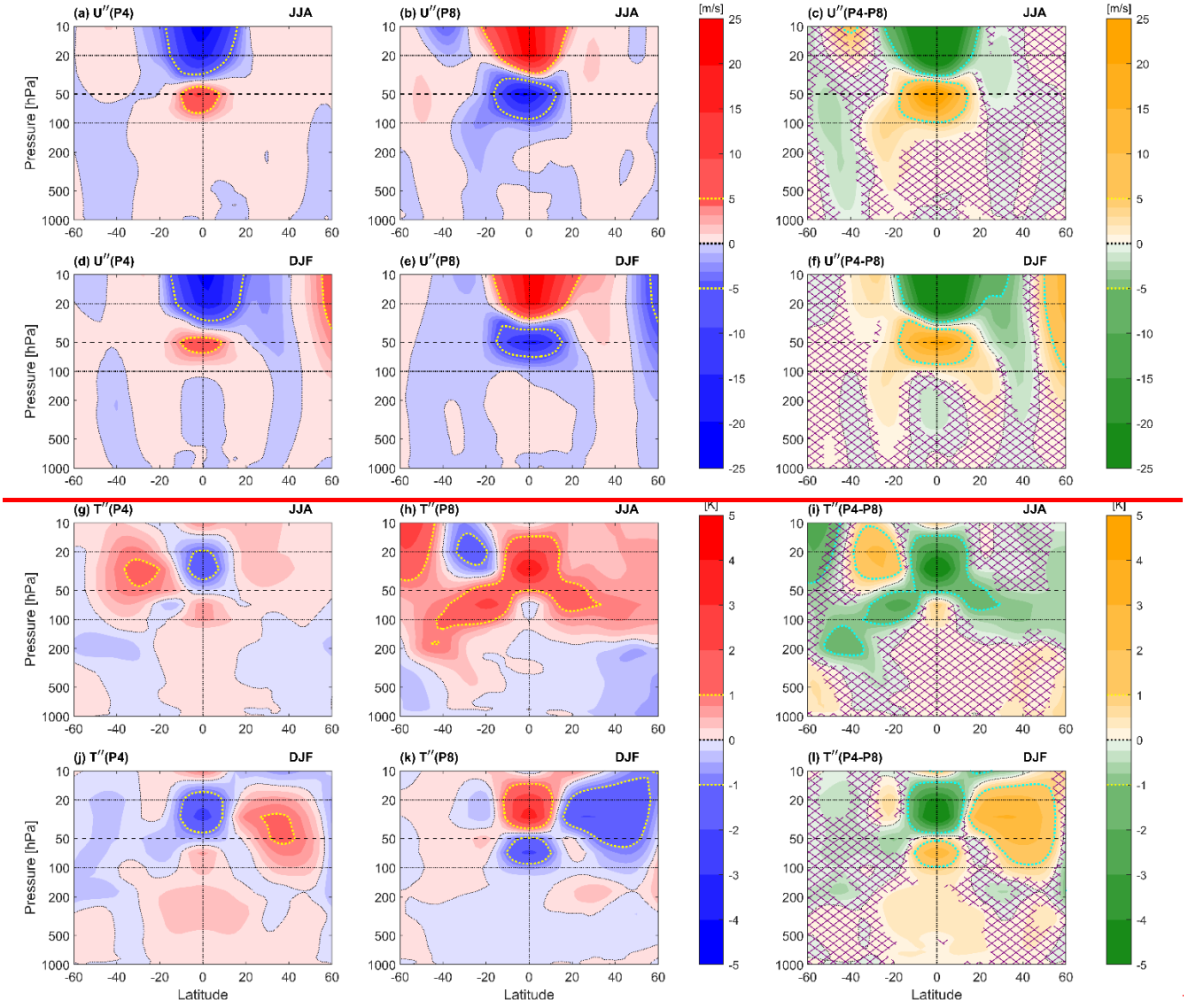

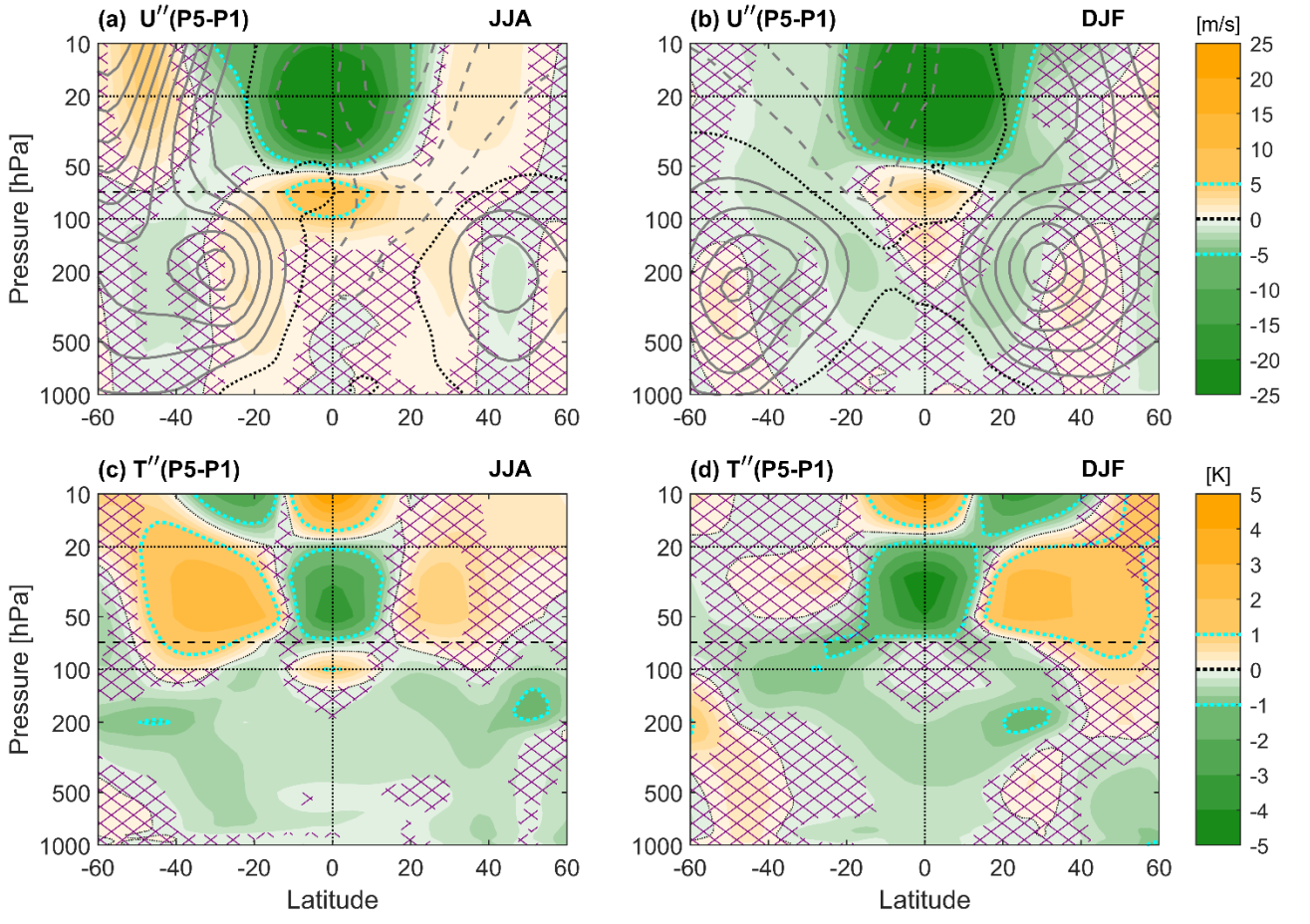

Figure 4. Same as Fig. 3, but for QBO W– E at 70hPa (P1–P5) and horizontal dashed is plotted for 70hPa level~~P5 (QBO W at 70 hPa) and P1 (QBO E at 70 hPa)~~.

The subtropical and extratropical tropospheric responses depend on season and phase of the QBO, with interesting differences seen even between using 50 hPa and 70 hPa as index levels (compare Figs. 3 and 4). For example, during DJF and QBO W at 70 hPa, a significant cooling anomaly is also evident in the lower troposphere poleward of 40°N (Fig. ~~4l~~4d). This confirms the recent finding of Kumar et al. (2024) regarding a ~~new~~ QBO teleconnection pathway for these cooling patterns via the UTLS region to the high-latitude surface which is independent of the H-T mechanism. Based on this zonal mean analysis, QBO dynamical teleconnections with tropical, subtropical, and polar regions vary with the seasons and downward propagation of the QBO anomalies. Additionally, the characteristics of QBO anomaly patterns in any latitudinal zone may differ with geographical location. Since the monsoon system is linked to the distribution of land and sea, and since ~~it~~ the climatological patterns associated with emanation of planetary wave trains are fundamentally zonally asymmetric, such as the PNA and NAO patterns, we now focus on the geographical variation of QBO teleconnections in the extratropics.

~~exhibits large geographical variations. Therefore, it is important to investigate the horizontal structure and variation of QBO teleconnections, therefore, from the next section onward, the analysis focuses on the non-zonal variations.~~

5. QBO teleconnections with the GM system

5.1 Composite differences of seasonal precipitation and surface wind for opposite QBO phases

In order to visualize regional effects of QBO dynamical teleconnections in the GM system, we investigated the horizontal distribution of the QBO signal~~anomalies~~ in precipitation and surface wind ~~for opposite phases of the QBO~~ during ~~the both~~ JJA and DJF (Fig. 5). The index pairs P4 – P8 (50 hPa index) and P5 – P1 (70 hPa index) are of interest since they are associated with significant QBO anomalies arriving in the tropical and subtropical UTLS. ~~The top row represents the composite difference QBO W – E of precipitation anomalies, overlain with significant (U", V") difference arrows at 950 hPa for the 50 hPa and 70 hPa indices (i.e., P4 – P8 and P5 – P1) during JJA, and bottom row same for DJF.~~ Significant patterns in the composite differences exist at continental scale in the equatorial, tropical, and extratropical regions which are related to modulation of regional atmospheric circulations for both seasons. As in the seasonal mean fields (Figs. 2b-c), one may observe a systematic association between precipitation maxima and convergence in anomalous surface wind patterns. The differences among the four panels in Fig. 5 illustrate that the regional monsoon system response to the QBO is sensitive to both season~~s~~ and QBO phase.

During JJA, deep convection shifts toward Southeast Asia, away from the Maritime Continent (Fig. 2b, d) and the South Asian High dominates the circulation in the UTLS. ~~During JJA and~~Applying ~~QBO W – E at~~the 50 hPa QBO index ~~(~~P4-P8 for JJA~~, Fig. 5a)~~, one may see enhanced precipitation near 20°N in the longitude band ~90°E - 180°E during QBO W (Fig. 5a). This is compatible with the UTLS cold anomaly in the rising branch of the QBO MMC seen near 20°N in Fig. 3c. At the equator there is enhanced precipitation near 135°E and reduced precipitation near 80°E and 170°E (Fig. 5a). The east-west dipole pattern modulates deep convection in the tropical west Pacific, which in turn affects the Pacific cell of the WC. One may interpret the pattern in Fig. 5a over the subtropical Northwest Pacific as an arc-shaped maximum during QBO W which occurs on the edge of the lower tropospheric anticyclone known as the Bonin High (Fig. 2b).~~an east-west dipole in precipitation is seen in the tropical sector ~ 120°E – 200°E (Fig. 5a). There is enhanced precipitation over Indonesia. This is likely due to differences in the spatial pattern of deep convection (Fig. 2b, d). During JJA, deep convection shifts toward South East Asia, away from the Maritime Continent. The South Asian High dominates the circulation in the UTLS. These differences in the basic state provide a different situation for the QBO MMC to interact, with modulation of convection occurring in different locations compared to DJF. The east-west dipole pattern modulates deep convection in the tropical West Pacific, which in turn affects the Pacific cell of the Walker Circulation (WC). QBO modulation of deep convection leads to modulation of the location and strength of lower tropospheric anticyclones in Bonin High (Fig. 2b), with QBO anomalies in the boundary layer circulation leading to changes in precipitation in subtropical region. For example, there is more rainfall in the Northwest Pacific during when there are QBO W at 50 hPa (Fig. 5a).~~ This represents an eastward shift in precipitation, with a negative anomaly over China and Southern Japan. Which is consistent with the results of Zhou et al. (2024), who showed that low precipitation

preferentially occurs in the ~~Yangtze Huaihe River Basin (~~YHRB~~)~~ during QBO W at 50 hPa. We will provide a detailed analysis of this point in a subsequent section. The composite difference QBO W– E at 70 hPa (P5-P1) for JJA ~~during NH summer monsoon JJA~~ does not show any significant ~~alterations~~ anomalies in precipitation or wind vectors ~~and only displays minor scale variations.~~ (Fig. 5b). However, reduced rainfall occurs over Indonesia during QBO W at 70 hPa, which is compatible with the QBO UTLS warm anomaly over the equator seen in Fig. 4c.

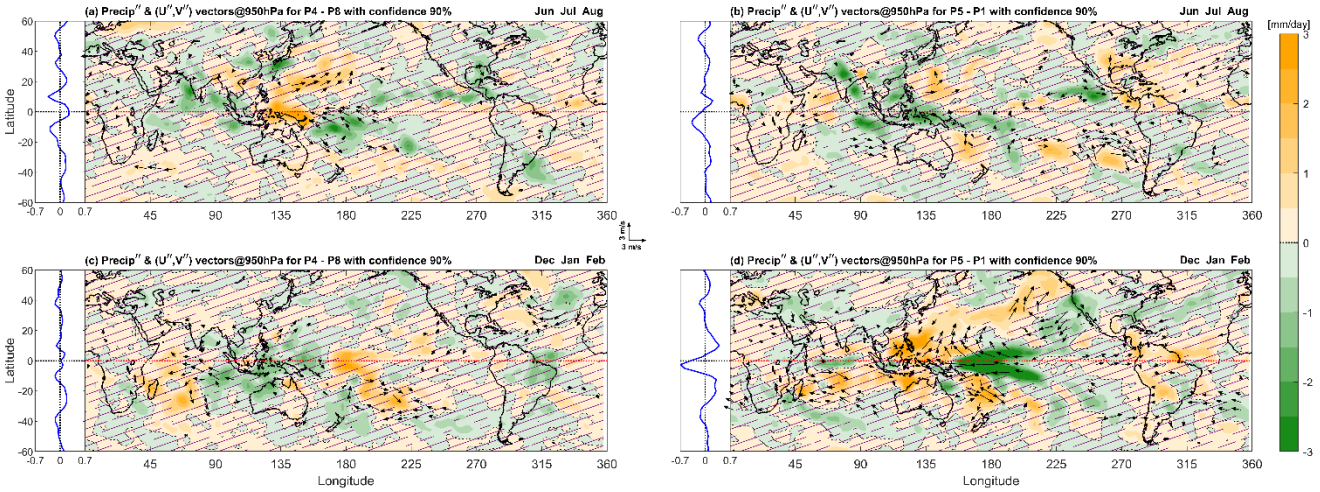

Figure 5. Longitude-latitude sections of QBO composite differences in precipitation (color bar) and 950 hPa horizontal winds (vector length shown in center inset) for QBO opposite phase pairs, for (a-b) JJA and (c-d) DJF. The left column represents QBO W – E at 50 hPa (P4 – P8), while the right column represents QBO W– E at 70 hPa (P5 – P1). The latitudinal profile of zonal mean precipitation is shown to the left of each panel. Wind anomalies (U'', V'') are plotted if either component's statistical significance exceeds 90%. Violet cross-hatching indicates regions of statistical significance less than 90%.

During DJF, convection over the Maritime Continent is more intense than during JJA and more symmetric about the equator (Fig. 2c). The SPCZ southeast of Indonesia is a significant zonally asymmetric region of off-equatorial heating during austral summer. The QBO W warm anomaly in the UTLS over the equator, obtained u~~U~~sing the 50 hPa index (P4-P8), is more robust than during JJA (compare Figs. 3d and 3c). This is accompanied by reduced precipitation over Indonesia (~90°E – 160°E) and in the SPCZ, with enhanced precipitation near the tropical date line (Fig. 5c). This is ~~one obtains the an opposite pattern in DJF (Fig. 5c) compared to JJA (Fig. 5a), the east-west dipole in the western tropical Pacific (~ 120°E – 200°E) switches sign, with less precipitation over Indonesia,~~ in agreement with previous results (Collimore et al., 2003; Tegtmeier et al., 2020; and Hitchman et al., 2021). QBO W at 50 hPa implies increased static stability in the tropical UTLS when there is a QBO warm anomaly near the tropopause (Gray et al., 1992b; Giorgetta et al., 1999). Consistent with this, Liess and Geller (2012) report a diminution of rainfall over Indonesia in DJF during QBO W. The reduced precipitation over Indonesia (Fig. 5c) is consistent with our zonal seasonal mean structure (Fig. ~~3~~l3d). As shown by Collimore et al. (2003), and discussed further below, there is local enhancement of the warm anomaly in the UTLS over Indonesia during DJF, compatible with the concept that convective positive feedbacks can amplify the response to QBO UTLS temperature anomalies.

During DJF, when the 70 hPa index (P5-P1) is used, the equatorial UTLS zonal mean warm anomaly in the troposphere seen in the 50 hPa index (Fig. 3d) becomes a cold anomaly in the upper troposphere (Fig. 4d). With the pattern of QBO MMC penetrating downward into the troposphere somewhat farther, in this phase precipitation is enhanced over Indonesia and suppressed near the date line (Fig. 5d). The response of convection in the tropical West Pacific during DJF is sensitive to QBO phases. ~~and non-zonal profile of tropopause structure shown later (Fig.6c), since that implies the existence of a warm anomaly near the tropical tropopause over the deep convective region of Indonesia. During The east-west dipole in the western tropical Pacific during DJF also switches sign when 70 hPa index, the pair P5 – P1 (Fig. 5d) is used instead of 50 hPa P4 – P8 (Fig. 5c). Along the equatorial region, the patterns resemble those of JJA for 50 hPa, exhibiting significant modulation in the Pacific cell of the WC and a dipole pattern in precipitation. However, the DJF patterns are broader with higher amplitudes. DJF~~ There is an enhanced anticyclonic circulation in the lower troposphere over the North Atlantic for the 50 hPa index (Fig. 5c) and over the Northeast Pacific for the 70 hPa index, with enhanced precipitation centered on the associated northward flow anomaly (Fig. 5d). The lower tropospheric regional circulations which are modulated by the QBO correspond to the NAO and PNA patterns, respectively. ~~also led to significant modulation in the extratropics, for 50hPa index, a significant modulation of precipitation (an east-west dipole) and wind vectors (semicircular anticyclonic circulation) can be seen over the North Atlantic Ocean (Fig. 5c), where the localized atmospheric circulation known as the Northern Atlantic Oscillation (NAO) prevails. For the 70 hPa index, the significant semicircular anticyclonic circulation and dipole pattern in precipitation over the Pacific North American (PNA) region further~~ This highlights that QBO dynamical teleconnections occur~~s~~ in regions where localized atmospheric circulations are present.

To explore ~~explore how~~ the zonal structure of UTLS QBO anomalies ~~behave in a non-zonal pattern near the tropopause and its possible teleconnection with GM system~~, ~~figure 6 shows composite QBO~~ composite differences ~~similar to Fig. 5, but~~ for ~~100 hPa~~ temperature and ~~100 hPa~~ horizontal winds at 100 hPa are shown in Fig. 6. During JJA, anomalous QBO W winds (range ~ 2-3 m/s) and a warm anomaly (range ~ 1-3 K) are found near the tropopause in a zonally-symmetric pattern along the equator. Using the 50 hPa index (P4-P8) the QBO W zonal wind anomaly at 100 hPa is larger than it is when using the 70 hPa index (P5-P1) (compare Figs. 6a, 6b). This is compatible with the downward progression and diminution of QBO W from Fig. 3a to Fig. 4a. The QBO temperature anomaly descends with time, being stronger at 100 hPa using the 70 hPa index than using the 50 hPa index (compare Figs. 3c and 4c). This is seen at 100 hPa as a narrowing of the westerlies and broadening of the temperature anomaly at the equator as the QBO MMC descend from the 50 hPa level to the 70 hPa level (compare Figs. 6a, 6b). This progression is also compatible with reduced equatorial precipitation as the warm anomaly enters the upper troposphere (compare Figs. 5a and 5b).

~~During JJA, anomalous QBO westerly~~ W ~~winds (range ~ 2-3 m/s) and a warm anomaly (range ~ 1-3 K) are found near the tropopause in a zonally-symmetric pattern along the equator. This is true for both the 50 hPa index level (Fig. 6a) and 70 hPa (Fig. 6b)~~ index levels~~, but the warm anomaly is more prominent for the 70 hPa index.~~ Note ~~also~~ the prominent QBO cold anomaly near 20°S during JJA, as shown by Hitchman et al. (2021). ~~;~~ I~~i~~t is associated with the same MMC which caused the warm anomaly over the equator~~, resulting in a stronger STJs in the SH winter~~ (Figs. 6a, b). The subtropical winter

cooling effect along the UTLS generated by the QBO MMC is stronger and more significant for the 50 hPa index (Fig. 6a). In agreement with the zonal mean structure during JJA, significant QBO negative temperature anomalies in the subtropics associated with the QBO MMC have zonally symmetric features in the winter hemisphere (Figs. 6a, b).

D~~In the NH summer~~uring JJA and~~,~~ using the 50 hPa ~~composite difference~~QBO index, one may observe ~~reveals~~ a distinct cool anomaly over the subtropical Northwest~~western~~ Pacific Ocean near 140°E (Fig. 6a) which extends into the Bering Sea and coincides with the region where a significant pattern was found in precipitation and wind vectors at the surface (Fig. 5a). Enhanced precipitation at the western edge of a weakened Bonin High may imply that more convective updrafts overshoot and cool the 100 hPa level in this region during QBO W. The composite difference for the 70 hPa index also shows a region of cooling in the subtropical lower stratosphere over the Central Pacific midlatitudes (Fig. 6b), although less robust than for the 50 hPa index. These results indicate that there are preferred longitude bands where the QBO can influence the extratropics along the subtropical UTLS, with subsequent modulation of extratropical surface weather.

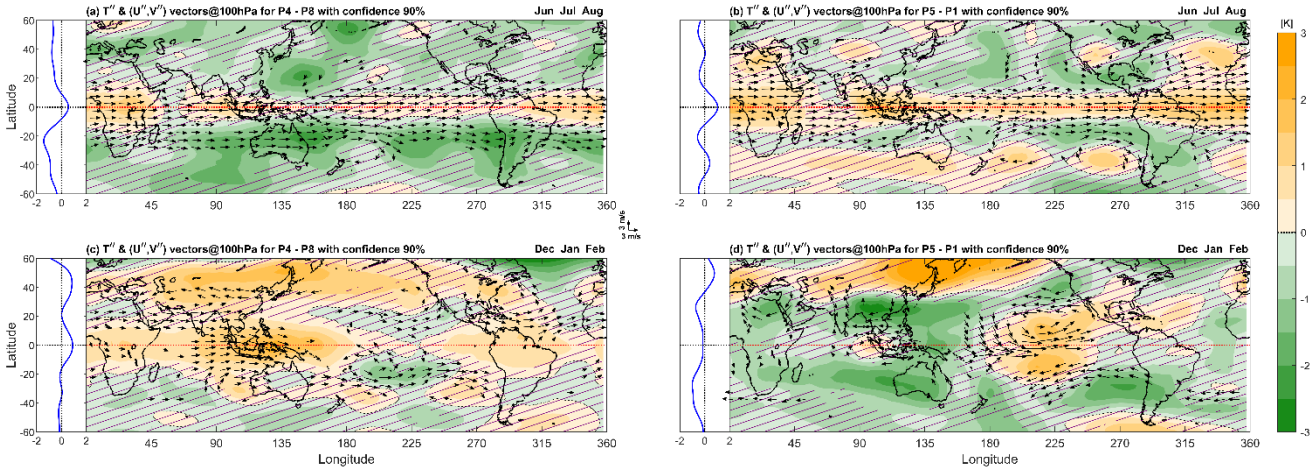

Figure 6. A~~Same as~~s in Fig. 5,~~Figure 5~~ but for temperature (~~T~~", (color bar) and wind vectors (U", V") at 100 hPa. The zonal mean meridional profile of QBO temperature anomaly is shown to the left of each panel.

During DJF the tropopause in convective regions usually lies above the 100 hPa level, making it harder for QBO wind regimes to affect the 100 hPa level. QBO westerly wind and warm temperature anomalies appear in the tropics at specific longitude bands (Figs. 6c, d). ~~, QBO westerly wind and warm temperature anomalies appear in the tropics at specific longitude bands (Figs. 6 c, d).~~ For the 50h Pa index, a significant QBO warm anomaly occurs over Indonesia, extending from Central Africa to the Date Line, with another warm anomaly over Amazonia (Fig. 6c). The range reaches 3K over Indonesia where significant westerly wind vectors reside. These warm anomalies coincide with the climatological locations of ~~chronic~~ deep convection, characterized by cloud top temperatures less than 192 K and low OLR emission (Collimore et al., 1998) and an easterly flow anomaly at 150 hPa, just below the tropical tropopause, consistent with a reduced WC during QBO W (cf. Figs. 18e, 19e of Hitchman et al., 2021). Similar temperature anomaly patterns were observed ~~by Hitchman et al. (2021)~~ in cold point tropopause temperature (CPT) for the same QBO W – E phases (~~see~~ Hitchman et al. 2021, ~~their~~ Fig. 17b). Tropical

UTLS thermal anomalies ~~associated with the monsoon system~~ are stronger during DJF, with greater geographical variation in the strength of deep convection and tropopause height. This creates a greater opportunity for QBO anomalies to preferentially affect regions with characteristically deep convection during DJF compared to JJA.

For 50 hPa index, ~~S~~significant QBO westerly wind anomalies can be seen in the NH and SH subtropical Eastern Pacific and in the North Atlantic (Fig. 6c), which was noted as downward-extending subtropical anomalies in the zonal mean structure (Figs. ~~3f~~3b). Extratropical QBO warm anomalies appear near 50°N and 30°S, being stronger in the winter hemisphere and, in the eastern hemisphere (Fig. 6c). A cold anomaly can be seen at 100 hPa centered near the tip of Greenland, consistent with an amplified wave-one pattern during QBO W (Kumar et al., 2024). This North Atlantic 100 hPa temperature anomaly is related to the westward shift in the precipitation maximum (Fig. 5c). This geographical fingerprint provides useful information for evaluating whether this teleconnection operates through the stratosphere pathway in the H-T mechanism or along the subtropical UTLS. Composite differences in 100 hPa temperature for QBO W – E at 70 hPa level shows a dipole pattern in the tropical Pacific and PNA regions, as was observed for the surface precipitation (Fig. 5~~-~~d). A wavenumber-1 pattern in temperature anomaly is also evident near 60°N (Fig. 6d), similar to that observed at 50 hPa (Fig. 6c). There are also significant easterly anomalies in the STJs of both hemispheres in the Eastern Pacific when the 70 hPa level is used, resulting in a cyclonic circulation anomaly off of the west coast of North America (upper level trough), which ~~is reverse to~~accompanies the anticyclonic surface wind vector anomaly in ~~(~~Fig. 5d~~)~~.

These composite differences maps illustrate the systematic, significant ~~modulations of the~~association between the GM system ~~by~~ and Q~~O~~BO anomalies in the UTLS~~, precipitation, and surface winds~~ throughout the tropics and extratropics. The characteristic of this dynamical teleconnection is regional and is manifested ~~in regions~~ where prominent localized atmospheric circulations prevail. Results are sensitive to QBO phase. In the tropics a QBO signal in precipitation is observed, which occurs in the centers of deep convection. The strongest signals are associated with modulation of the Pacific component of the WC and exhibit significant dependence on season and on QBO index level. The zonal mean QBO MMC causes simultaneous antiphased cold and warm anomalies in the tropical and subtropical UTLS. In the tropics the QBO modulates regions of deep convection and therefore creates a regionally-varying signal which can also propagate into the extratropics along the UTLS. The manner in which the teleconnection signal propagates from the tropics into the midlatitudes is not fully understood but involves modulation of planetary Rossby wave radiation from tropical convective centers. Locally this can lead to changes in seasonal mean cyclonic and anticyclonic circulations in the extratropics~~, thereby leading to enhanced or diminished local meridional overturning in "local Hadley cells"~~. During the NH summer the stratospheric route is disabled. Therefore, during summer~~,~~ the QBO can only~~primarily~~ influence~~s~~ the extratropics via the subtropical UTLS pathway, but during winter a QBO teleconnection can reach the extratropical surface via either the stratospheric pathway and annular modes or via the subtropical UTLS. The rest of this study will investigate precise information on these potential routes with their regional characteristics.

5.2 QBO dynamical teleconnection with the Northwest Pacific during JJA

In order to investigate dynamical teleconnections operating along the subtropical route during boreal summer JJA, we analyze composite climatologies of precipitation and other meteorological parameters, for QBO W and E phases at 50 hPa (P4 and P8), along with composite differences. The Northwest Pacific region (10°-50°N, 120°-190°E) is shown in Fig. 7 ~~during JJA for the 50 hPa QBO index (P4 and P8)~~. From top to bottom, rows show precipitation, 500 hPa ~~vertical~~ W- wind ~~(W)~~, MLSP together with 950 hPa horizontal winds, and ~~100 hPa~~ temperature together with ~~100 hPa~~ horizontal winds at 100 hPa. The presence of the QBO signal is clearly visible even in the composite climatologies for QBO W and E phases (P4 and P8). During QBO E at 50 hPa, the band of precipitation which arches anticyclonically toward Alaska is enhanced south of Japan (Fig. 7b), with associated increase in mid-tropospheric upward motion (Fig. 7e). During QBO W at 50 hPa there is less precipitation along this summertime synoptic-scale storm track, more precipitation throughout the rest of the Northwest Pacific (Fig. 7a), and reduced upward motion near the southern tip of Japan (Fig. 7d). These features are more easily seen in the difference plots (~~P4 – P8,~~ Figs. 7c, f).

This variation in precipitation is associated with modulation of the regional circulation (Figs. 7g-l). During QBO W at 50 hPa, the lower tropospheric anticyclonic which dominates the Northwest Pacific basin is diminished (Fig. 7g), while it is enhanced during QBO E at 50 hPa (Fig. 7h), such that a negative anomaly in MSLP and cyclonic anomalous circulation is seen in the difference composite QBO W – E (Fig. 7i). During the QBO W phase the high-pressure region contracts, with isobars shifting slightly eastward (as indicated by the position of the yellow line in Fig. 7g). This shrinking of the ~~high pressure zone~~western edge of the surface anticyclone allows for the eastward expansion of convective precipitation from south of Japan into the Northwest Pacific during QBO W. Diminution of the anticyclone is accompanied by anomalous upward motion at 500 hPa in the Northwest Pacific and decreased upward motion south of Japan during QBO W (Fig. 7f). ~~is associated with diminished northward flow towards Japan. The resultant change in the anticyclone circulation will bring less precipitation over south of Japan and along the periphery of the anticyclone, with enhanced precipitation in this region during QBO E.~~ The reduction of the surface anticyclone during QBO W compared to QBO E may be seen in Figs. 7g, h, with anomaly vectors in Fig. 7i showing reduced anticyclonic flow during QBO W. At 100 hPa over the Northwest Pacific the air is cooler during QBO W (Fig. 7l). During QBO W there is more convection over ~~Heavy precipitation is associated with rising air currents; therefore, the vertical wind should be stronger over such areas. These upward winds do not remain limited within planetary boundary layers and penetrate beyond the mid troposphere into the upper troposphere (Fig. 7f). At 100 hPa, it can be seen that~~ the Northwest Pacific ~~region~~ during JJA, which is accompanied by reduced lower tropospheric anticyclonic flow and a colder UTLS.

This region is influenced by the northeast portion of the ~~is dominated by the northeastern portion of the~~ South Asian High ~~, which dominates the lower stratospheric circulation in the subtropics from the Western Pacific westward to the Atlantic Ocean~~ (Figs. 7j, k, l). Note the strong anticyclonic curvature of the flow near 30°N, 120°E. During QBO W at 50 hPa this circulation is stronger, with an associated cold anomaly at 100 hPa (Fig. 7j), while during QBO E this circulation is weaker and 100 hPa temperatures are not as cold (Fig. 7k). ~~This results in composite difference fields such that the high cold~~

~~anticyclonic dome extends upward further into the stratosphere~~ D~~d~~uring QBO W this results in~~, with~~ enhanced southward flow in the central North Pacific on the eastern edge of the ~~QBO anomaly~~South Asian High (Fig. 7l).

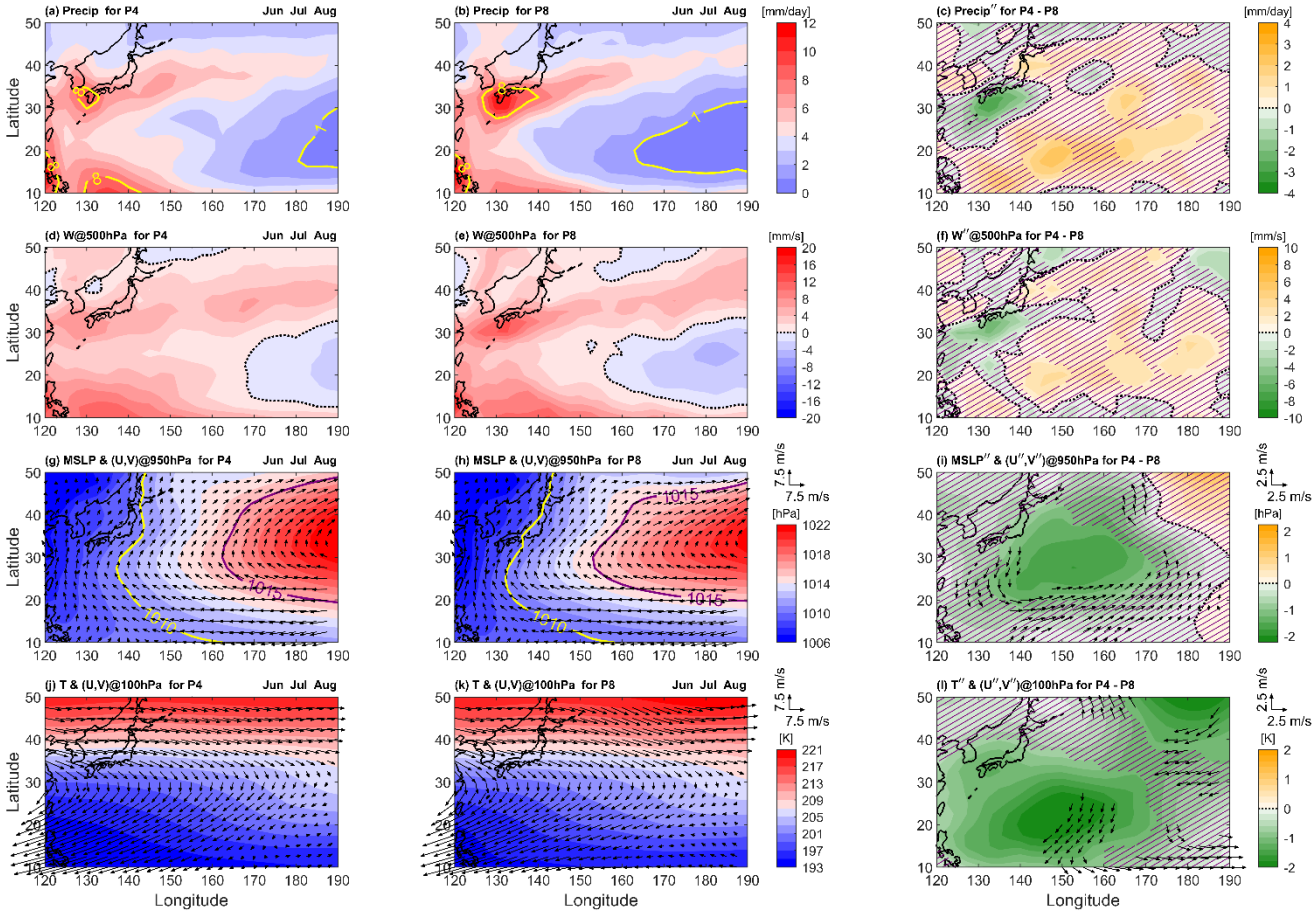

Figure 7. QBO regional teleconnection manifestation in the Northwest Pacific (10°-50°N, 120°-190°E) during boreal summer (JJA), showing composite climatolgies for ~~QBO phases~~ (left) QBO W at 50 hPa (P4), (middle) QBO E at 50 hPa (P8), and (right) QBO W- -E at 50 hPa (P4-P8), for (a-c) precipitation, (d-f) mid tropospheric W--wind at 500 hPa, (g-i) MLSP with (U, V) wind at 950 hPa, and (j-l) 100 hPa temperature with (U, V) wind. The violet cross hatching on the composite difference plots indicates regions of statistical significance less than 90%. Wind anomalies (U'', V'') are plotted only if either component's statistical significance exceeds 90%.

D~~As shown in Fig. 6a,~~uring JJA a significant QBO cold ~~MMC signal~~anomaly was found at 100 hPa over ~~this region only~~the Northwest Pacific during QBO W at 50 hPa (Figs. 6a, 7l), with~~and~~ a ~~composite differences in 100 hPa temperature anomalies show similar significant patterns~~reduced anticyclone in~~as~~ MSLP and 950 hPa winds ~~, but on a larger scale~~ (Fig. ~~7~~7i~~l~~). Postel and Hitchman (1999, 2001) showed that there is a maximum in Rossby wave breaking in the UTLS (150 hPa) in JJA in this region associated with the episodic detrainment of low potential vorticity from the Tibetan High in the upper troposphere northeastward over the Pacific. These events occur when transient synoptic waves travel along the poleward edge of the South Asian High. This regional maximum in Rossby wave breaking (RWB) was confirmed by Hitchman and Huesmann

(2007) for the 350 K surface. The South Asian High appears to be more robust in its northeast quadrant during QBO W at 50 hPa. This analysis suggests that, in the ~~subtropical route~~UTLS pathway, the QBO can connect to surface dynamics at a regional scale via modulation of localized atmospheric circulations.

5.3 QBO teleconnections with the North Atlantic during DJF for 50 hPa index

Figure 8 is in the same format as Fig. 7, but focuses on the North Atlantic region (20°-60°N, 280°-350°E) ~~during~~ for ~~austral summer~~boreal winter. During DJF, teleconnection ~~pathways~~ routes are possible, via either the stratosphere, or along the UTLS, or both. For QBO W at 50 hPa (Fig. 8a), precipitation is enhanced in the Western North Atlantic and diminished in the eastern North Atlantic relative to QBO E (Fig. 8b). This feature is distinctly recognizable as a significant east-west dipole in the composite difference QBO W – E (Fig. 8c), indicating a westward shift in precipitation during QBO W. A similar east–west dipole pattern is also evident in ~~the~~ anomalous vertical motion at 500 hPa, reflecting a westward shift in upward motion during QBO W (Fig. 8 f). The variation in precipitation is closely linked to changes in the GM system circulation patterns (Figs. 8g-l). During QBO W at 50 hPa, the dominant Azores High surface anticyclone is strengthened (Fig. 8g), with a westward shift in poleward advection of moist tropical air. This signal is quasi-barotropic, extending from the surface to the lowest stratosphere at 200 hPa (Fig. 8l). It represents a strengthening of anticyclonic flow in the North Atlantic during QBO W at 50 hPa. A stronger Azores High implies a higher index NAO and stronger ~~northeastward~~ flow ~~toward~~ into ~~Scandinavia in the northern North Atlantic~~northern Europe (e.g., Thompson and Wallace 2000).

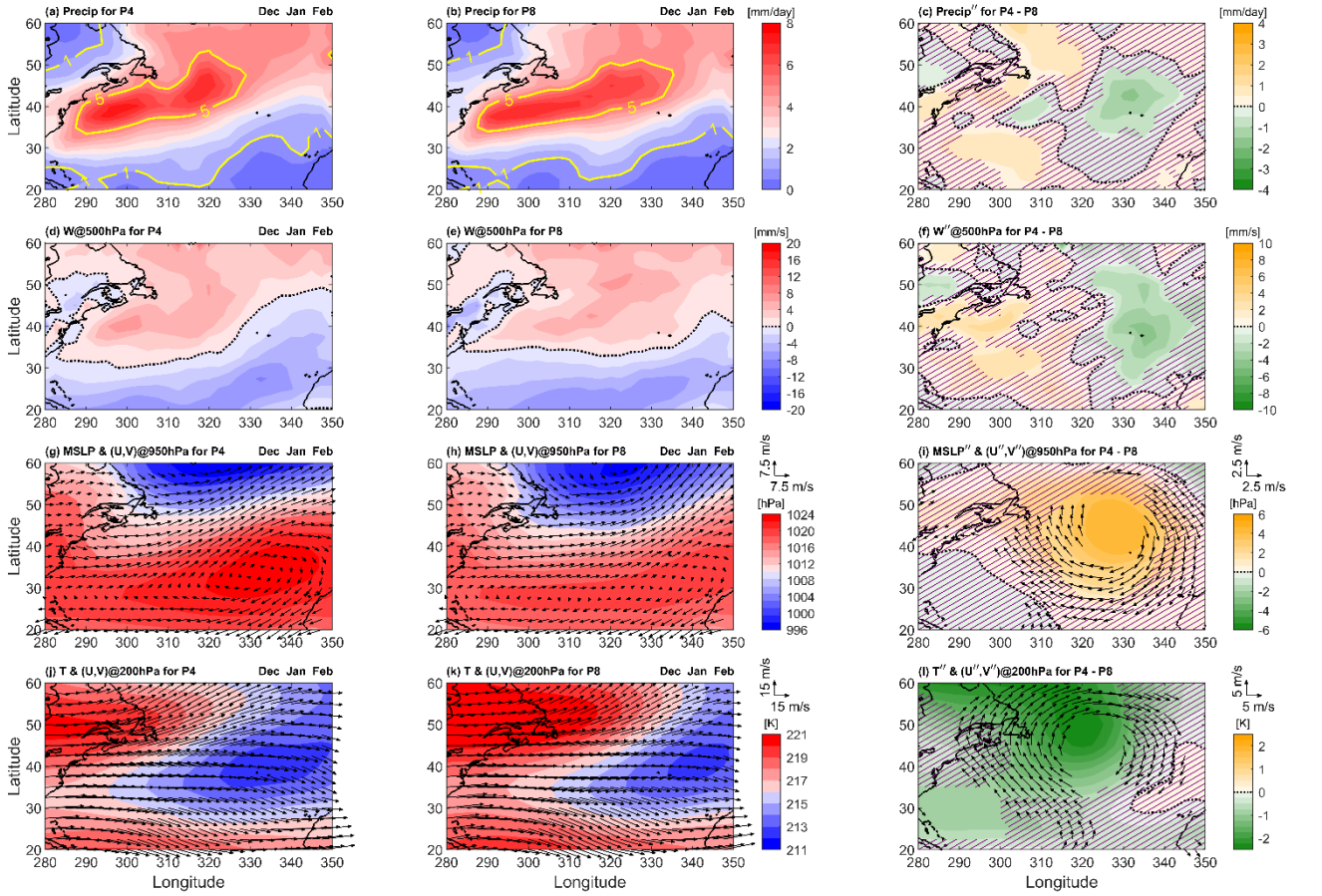

Figure 8. As in Fig. 7, but for DJF and focused over the North Atlantic Ocean (20°-60°N, 280°-350°E).

The increased pressure in the Azores High enhances the anticyclonic circulation near the Azores, resulting in a more intense North Atlantic (NA) jet stream. This change in anticyclone creates optimal conditions for heavy precipitation in the western NA including the eastern coast of North America and lighter precipitation around the Azores High (Fig. 8a). The opposite effect~~scenario~~ is found for QBO E at 50 hPa (Fig. 8b). The composite difference QBO W – E clearly highlights this feature, showing ~~a~~ significant anticyclonic motion in wind anomalies centered around the high ~~-~~pressure zone (Fig. 8i). Similar to JJA, stronger upward motion can be observed at 500 hPa (Fig. 8d to f) over regions of ~~heavy~~ enhanced precipitation.

In the extratropical lower stratosphere (200 hPa), temperature anomalies display significant patterns akin to those of MSLP (Figs. 8i, l). This is contrast to the situation in the Northwest Pacific during JJA, where a large surface anticyclone is centered over the Pacific and a larger anticyclone is centered over Tibet in the UTLS (Figs. 7i, l). In the North Atlantic during DJF the structure is equivalent barotropic, with a strengthened anticyclone extending upward, causing cooling of the lower stratosphere in the eastern North Atlantic during QBO W at 50 hPa (Fig. 8i, l). ~~A similar relationship is seen between the strengthened northeastward extension of the South Asian High and the cold anomaly at 100 hPa during QBO W in JJA (Fig.~~

~~7)~~. As discussed earlier in the seasonal DJF zonal mean structure for the 50 hPa index, these anomaly patterns may be linked to either the H-T mechanism associated with the stratospheric QBO teleconnection route, or to the route along the subtropical UTLS, or to a combination of both. T~~But, again refining that t~~he influence of the QBO is manifested ~~at a regional scale~~ where ~~localized~~ regional atmospheric circulations exist. In this case, the QBO is regionally interacting with the NAO.

5.4 QBO teleconnections with the Northeast Pacific during DJF for 70 hPa index

Figure 9 shows the same variables as in Fig. 8, but for the northeast Pacific region (20°-60°N, 190°-260°E) and using the 70 hPa index. ~~QBO interacts with the PNA pattern for 70 hPa index.~~ During QBO W, rainfall ~~is enhanced with along~~and 500 hPa vertical motion are both enhanced ~~(Fig. 9 a, d)~~ from northwest of Hawaii to the Gulf of Alaska, while these are diminished along the west coast of the United States (Fig. 9c, f). ~~The opposite effects can be seen during the QBO E phaseThe reverse scenario during can be seen during the QBO E phase.~~

Consistent with ~~previous~~ results from ~~(~~sections 5.2 and~~&~~ ~~5.4~~5.3~~)~~, these patterns are systematically linked with variations in the localized atmospheric circulations. QBO W at 70 hPa modulates the tropospheric planetary wave pattern in this region such that a positive PNA pattern is excited, with an enhanced surface low in the Gulf of Alaska and enhanced anticyclonic flow off the west coast of California (Fig. 9i~~g~~). A stronger tropospheric low in the Gulf of Alaska implies a lower tropopause, hence a warm anomaly in the lower stratosphere near 200 hPa (Fig. 9l). The effect of the QBO on the PNA is similar to that of ENSO, where QBO W at 70 hPa (or La Nina) favors more precipitation in Alaska, while QBO E at 70 hPa (or El Nino) favors more precipitation in California during DJF. Note that our analysis includes only the neutral ENSO phase.~~,~~ We~~ and~~ obtain~~ed~~ very similar~~the same~~ patterns ~~even with a low~~using the lower threshold values of ±0.4 K of the ENSO index (Fig. S3) ~~(±0.5 K)~~. ~~Therefore, any contamination from ENSO events can be ruled out.~~

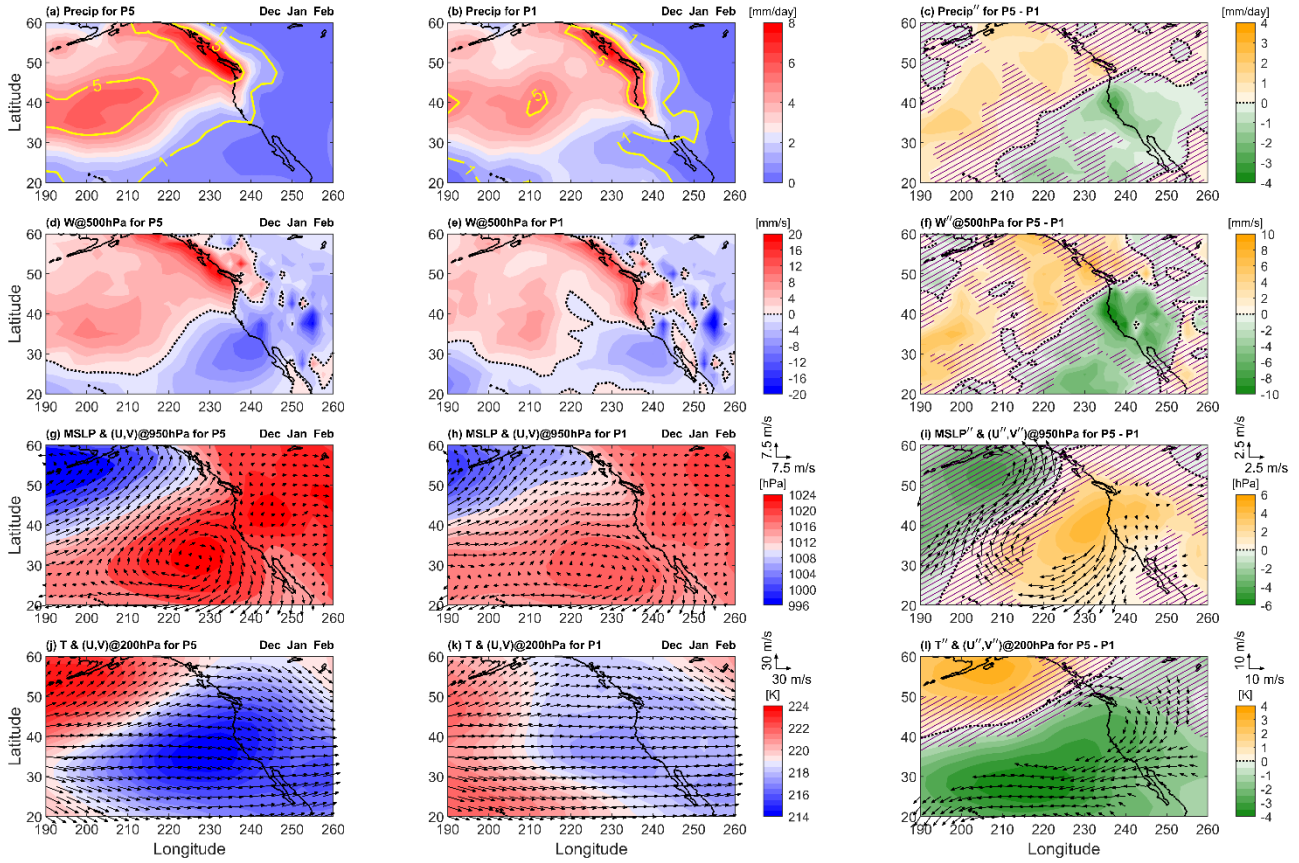

Figure 9. As in Fig. 7, but focused over the Northeast Pacific region (20°-60°N, 190°-260°E) during DJF, for QBO W and E at 70 hPa (P5 and P1).

6. Longitude-altitude structure of regional QBO anomalies

The above analysis suggests that the QBO has dynamical teleconnections with different parts of the GM system via modulation of regional atmospheric circulations. The anomalies in MSLP, surface winds, and precipitation patterns were found to be associated with QBO ~~footprint~~ anomalies in the UTLS. To better understand the vertical structure of perturbations associated with the QBO, we analyze longitude-altitude sections of anomalies in ~~geopotential height (~~GPH~~)~~, ~~zonal~~ vertical ~~wind~~ shear of zonal wind, temperature, static stability, meridional wind, and vertical wind. These analyses are averaged over selected latitude bands for the ~~the opposite~~paired QBO phases at which significant composite difference patterns were observed for three regions: the Northwest Pacific during JJA, the North Atlantic Ocean during DJF, and the Northeast Pacific during DJF (Fig. 10).

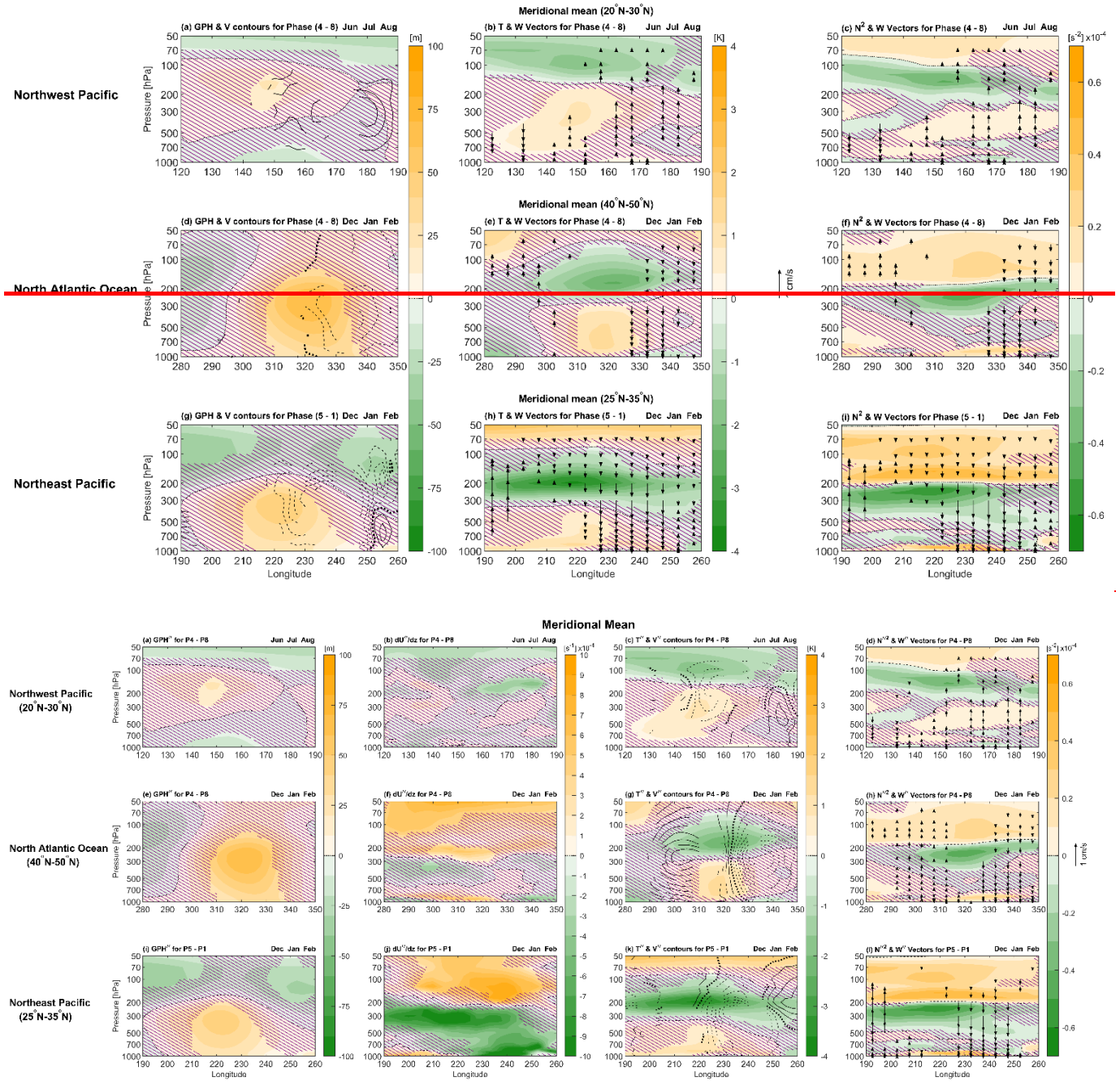

Figure 10. Longitude-pressure sections of composite differences between opposite QBO phases for selected latitudinal means shown in Fig. 7, 8, and 9. The top row shows the latitudinal mean between 20°N and 30°N over the Northwest Pacific (120°E - 190°E) during JJA, the middle row shows the mean between 40°N and 50°N over the North Atlantic Ocean (280°E – 350°E) during DJF, and bottom row shows the mean between 25°N and 35°N over Northeast~~Eastern~~ Pacific (190° E ~~W~~ and 260° E~~W~~) during DJF. The first, second, third, and ~~third~~ fourth column of each row represent the composite difference of GPH'' ~~(color bar) and V'' wind (contour lines)~~, vertical shear of zonal wind (dU/dz), T′′ (color bar) V'' wind (contour lines at 0.5 m/s)~~with W'' wind vectors~~, and N''^{2} with W'' wind vectors, respectively. The top two

rows use QBO W – E at 50 hPa (P4 – P8), and the third uses 70 hPa indices (P5 – P1). ~~5N~~Violet cross-hatching indicates regions of statistical significance less than 90%. The V" contours on the ~~1st~~ 3rd column and W" wind arrows on the ~~2nd~~ 4th ~~and 3rd~~ column are plotted only if only if either component's statistical significance exceeds the 90%. ~~their statistical significance exceeds 90%. I~~

In the Northwest Pacific during JJA, the composite difference in GPH anomaly shows low values over the region ~~(~~135°E – 170°E (Fig. 10a),~~)~~ where ~~a~~ diminution of the ~~surface~~ lower tropospheric anticyclone and strengthening of the upper tropospheric anticyclonic flow is~~was~~ observed during QBO W. This upper tropospheric ridging is compatible with our finding that there is a northeastward extension of the South Asian High into the region (Figs. 7c, f, i, l). It is also compatible with more convection in the Northwest Pacific. Above 150 hPa one may see the subtropical UTLS cold anomaly anomaly, which may help promote deep convection in this region during QBO W (Fig. 10c). ~~without any significant changes in vertical shear (Fig. 10b)and cold anomaly in the lower stratosphere (Fig. 10b). The stratospheric low GPH anomaly is associated with negative shear andthe cool anomaly (Fig. 10b, c).~~ Indeed, static stability is reduced in the layer 150 – 70 hPa and there is enhanced upward motion throughout the troposphere during QBO W in this region (Fig. 10d). The QBO anomaly in meridional wind shows anomalous poleward flow to the west and equatorward flow to the east of this enhanced anticyclonic flow in the UTLS during QBO W (Fig. 10c). This represents an amplification of the time mean flow in the RWB surf zone to the northeast of the South Asian High (Postel and Hitchman 1999). ~~Interestingly, the tropospheric warming patterns are limited in longitudinal range where significant modulation was observed in the MSLP. The static stability (Brunt Väisäläväisälä frequency) patterns shows a statistically significant alternating tripole patterns: positive in stratospheric region (above 70 hPa), negative around the tropopause (200 hPa– 100 hPa), and positive in the mid tropospheric region (700 hPa – 300 hPa) (Fig. 10c10d). In the upper troposphere, the enhanced northeastward extension of the South Asian High during QBO W can observed as a high GPH anomaly (Fig. 10a), with reduced static stability above (Fig. 10c10d). Significant upward motion anomaly in the entire anomalies at the upper troposphere can also be seen (Fig. 10c10d), with significant limited positive v wind contours representing the meridional circulations on the northward side (Fig.10a10c). These systematic modulations from tropospheric to stratospheric region, as well as the meridional linkage, suggest the possible role of the QBO in modulating precipitation and other meteorological variables in regional circulation systems.~~

Zhou et al.~~at el.~~ (2024) analysed the QBO meridional structure averaged over 120°E-160°E for ~~the summer monsoon,~~ JJA~~,~~ and showed that during QBO W at 50 hPa there are regional zonal wind anomalies in the troposphere in the band 30°N-40°N, This corresponds to an equatorward shift in the STJs during QBO W, which coincides with reduced moisture transport and convergence, leading to lower rainfall extremes in the YHRB. Gao et al. (2023) described these results in terms of a regional QBO MMC anomaly. Our results confirm low precipitation over this region for QBO W at 50 hPa, but these features are not limited to the YHRB, having broader spatial domains spanning the Northwest Pacific.

In our analysis, we found a regional cool anomaly in the upper troposphere over the Northwest Pacific during QBO W at 50hPa. This is related to enhanced deep convection in the Southeast Asian monsoon, the northeastward expansion of the South Asian High in the upper troposphere, and diminution of the surface anticyclone over the Northwest Pacific. These changes result in reduced upward motion and precipitation over the southern tip of Japan and enhanced upward motion and

precipitation over the Northwest Pacific. It is possible to call this a local MMC anomaly, where the polarity is rising over the Northwestern Pacific and sinking over Japan during QBO W at 50 hPa, but the underlying cause for this apparent local circulation is more complex.

Considering the zonal mean temperature anomalies in Fig. ~~3i~~3c, one may see a QBO cold anomaly all along the subtropical UTLS during QBO W at 50 hPa, which accompanies the warm anomaly over the equator. The zonal mean QBO cold anomaly in the subtropics is caused by a rising branch of the QBO MMC, while the warm anomaly is caused by the sinking branch in the tropical UTLS. This subtropical cold anomaly might be expected to enhance precipitation in a zonally-symmetric pattern, since there is a decrease in static stability in the subtropical UTLS across Asia and the Northwest Pacific, from 120°E to 180°E (Fig. 10c). This would encourage more deep convection over the Northwest Pacific relative to over land along the east coast of Asia during QBO W. Another aspect of this system which may be important in this context is that deep tropical convection is suppressed over Indonesia during QBO W, which implies reduced subtropical downwelling. The lower tropospheric anticyclone which dominates the circulation east of Japan during summer (the Bonin High, Enomoto et al., 2003) is one region of subsidence ~~in such a local Hadley Cell~~. With reduced convection in the adjacent tropics, one might expect a reduction in subsidence and strength of the Bonin High~~, which is observed (Figs. 7f, i and 10a)~~. In our analysis, the reduced subtropical downwelling is evident as a significant upward W-wind anomaly accompanied by notable meridional wind contours, suggesting a weakening of the region of subsidence over east of Japan (Fig. 10c, d).

To see other possible routes for QBO dynamical teleconnection, potentially through the polar or extratropical region, orthographic NH polar projections (0°N–90°N) of GPH" at 50 hPa, along with 200 hPa tropospheric temperature, MSLP, and precipitation, are shown in Fig. S3 S4 for JJA. None of the panels exhibit any other possible routes for QBO teleconnections at the 50 hPa level (2nd column, Fig. S3S4) or even at 70 hPa (3rd column, Fig. S3S4), because quasi-stationary planetary wave activity between the equator and polar regions remains very low during the summer monsoon season when stratospheric winds are easterly (Chen et al., 2005). The orthographic polar projections also highlight the localized characteristics of the QBO MMC subtropical UTLS route over the Northwest Pacific, as previously discussed.

During DJF, the nature of dynamical teleconnection remains intact across ~~with the downward propagation of the~~ QBO phases ~~(~~50hPa to 70hPa), but the geographical location for surface linkage changes. For both the ~~regions,~~ North Atlantic ~~Ocean during DJF~~ and Northeast Pacific, ~~the~~ significant positive GPH anomalies prevail~~s~~ ~~(Fig. 10e, i)~~ in the ~~entire~~ troposphere, but the Atlantic anticyclonic anomaly extends upward above 300 hPa (Figs. 10e, i). The locations of these anomalies coincide with the locations of the anticyclonic MSLP anomalies in Figs. 8i and 9i. In both regions there is a negative wind shear anomaly in the troposphere and a positive shear anomaly in the lower stratosphere (Figs. 10f, j), but with significantly larger magnitudes over the Northeast Pacific. During DJF we found a regional cool anomaly in the upper troposphere off the coast of California, with a warm anomaly in the Gulf of Alaska during QBO W at 50 hPa (Fig. 9l). The cold anomaly at 25-35°N may be seen in Fig. 10k. The vertical structure of QBO temperature anomalies is similar in both the Atlantic region and off the coast of California, with a cold anomaly in the lower stratosphere (above 300 hPa) and warm anomaly throughout the

troposphere (Figs. 10g, k). This implies changes in static stability, with a decrease below 200 hPa and an increase above (Fig. 10h, j).

These anticyclonic anomalies during QBO W are accompanied by anomalous rising poleward motion to the west and equatorward sinking motion to the east (Figs. 10g, h, k, l). ~~tropospheric region but within respective longitudinal range where significant composite difference was found in the MSLP (Fig. 8i10d and 9ig). The Atlantic patterns are vertically deeper in compare to Pacific. Interestingly, temperature anomalies of both regions reflect the significant dipole pattern; positive anomalies in the tropospheric region below 300hPa and negative in upper tropospheric region from 300hPa to 100hPa (Fig. 10g e and kh). The static stability also exhibits a significant dipole pattern centered around the peak amplitude of negative anomalies in the temperature dipole pattern ~200 hPa.~~ During DJF, ~~,~~ between 40°N and 50°N in the North Atlantic, the climatological vertical motion field exhibits marginal ascent over the oceanic eastern sector and marginal subsidence over the continental western sector (see Fig. 2a of Schwendike et al., 2014). Therefore, QBO at 50 hPa reduces the contrast between these ascending and descending branches.

To better understand QBO teleconnections during DJF, ~~-~~we also examined orthographic NH polar projections (0°N–90°N) of GPH" at 50 hPa, along with 200 hPa temperature, MSLP, and precipitation (Fig. 12). ~~To better understand QBO teleconnections during DJF, we also analyzed the horizontal distribution of various dynamical parameters on orthographic NH polar projections (0°N–90°N), which are shown in Fig. 11.~~ Over the Arctic Circle (> 60°N), significant composite differences, QBO W – E (P4 – P8), are seen in GPH″ at 50 hPa, ~~are~~ indicative of a deeper polar vortex during QBO W than QBO E (2nd column Fig, ~~10~~ 11a). This annular mode structure is part of the teleconnection pathway originally known as the QBO stratospheric route, or H-T Mechanism. The lower stratospheric T″ anomalies at 200 hPa are somewhat similar to those at 50 hPa GPH″ (2nd column Fig. ~~10b~~11b), consistent with a deeper and cooler polar vortex during QBO W. ~~However,~~ MSLP″ also shows a low anomaly over the pole, but it is not significant (Fig. 11c). However, the amplification of the surface anticyclone and reduction in rainfall over the North Atlantic during QBO W are significant (Figs. 11c, d).~~patterns are rather independent from GPH″ (2nd column Fig. 10c11c), showing the association with NAO as discussed in section 5.2.~~ The NAO and polar vortex are linked by annular mode structures (Kodera et al., 1999, Kumar et al., 2022). The QBO-NAO teleconnection may result from tropospheric eddies interacting with barotropic annular anomalies (Kushner 2010). This can result in ~~QBO-induced changes in the tropospheric circulation anomalies via the downward control principle (Haynes et al., 1991), and zonal flow - stationary wave interactions. Another possible mechanism for this teleconnection may be associated with QBO~~ latitudinal displacement of the STJs (Fig.3b). Factors which can affect the response include nonlinear interaction between the STJ and polar night jet (PNJ) (Kushner and Polvani, 2004) and the presence or absence of strong zonal asymmetries (Gerber and Polvani, 2009). The relationship between zonal mean QBO anomalies associated with the QBO MMC and regional circulations is complex, with distinctly different responses of the local STJs over the Pacific and Atlantic and during DJF and JJA (Kumar et al., 2022). However, a detailed mechanism for the NAO- QBO dynamical teleconnection is still unclear and needs to be explored in the future.

For the 70 hPa index pair~~r~~ P5 – P1~~, the location of~~ statistically significant QBO modulation ~~shifts from the North Atlantic to the~~is found in the Northeast Pacific (Fig. 11, right-hand column)~~, but the characteristic nature of vertical coupling is found to be similar in both the regions (compare 2nd and 3rd rows of Fig. 10)~~. ~~In the longitude altitude structure, the significant negative v-wind contours representing the meridional circulations on the southward side with downward wind (Fig.10g, h).~~ The composite difference QBO W– E for ~~at 70 hPa (P5–P1) of~~ GPH″ does not reflect any annular mode structure. This may argue against the H-T mechanism but it is possible for annular modes to interact with the flow to yield a large ridge over the North Pacific. ~~,~~ It is also highly possible that the PNA pattern is altered via the UTLS pathway, which leads to a stronger Aleutian High. Climatologically, during DJF the Aleutian High tilts westward with height from the troposphere into the upper stratosphere and mesosphere (Harvey and Hitchman 1996). ~~i.e. no H–T mechanism.~~ This ~~Instead, a~~ wave-number-one ~~-~~pattern~~s exists~~ (3rd column in Fig. 11a), ~~with~~ consists of an amplified Aleutian High~~h~~ over the Pacific and trough over the North Atlantic ~~(Harvey and Hitchman 1996) during QBO W at 70 hPa and DJF~~. Although the trough anomaly is not highly significant, the Aleutian High anomaly is. The lower stratospheric temperature patterns at 200 hPa are consistent with GPH″, where a warm anomaly underlies the Aleutian High amplification~~ed anomaly~~ over the North Pacific and a cold anomaly underlies the trough over the North Atlantic. ~~and a cold anomaly underlies the trough over the North Atlantic. This ridge-trough pair tilts westward with height from the troposphere into the upper stratosphere and mesosphere (Harvey and Hitchman 1996). Thus, the QBO can modulate this fundamental structure.~~ When the 70 hPa index is used during DJF one may also see a strongly amplified Siberian High in the high latitude sector~~Interestingly, a significant MLSP anomaly lies in Arctic Circle as a semi-disc structure~~ ~~(~~0°E–180°E and reduced precipitation in Northern Eurasia (Figs. 11c, d, 3rd column)~~)~~. ~~, along with some significant patterns in the northeastern Pacific region which modulates the PNA as discussed above~~.

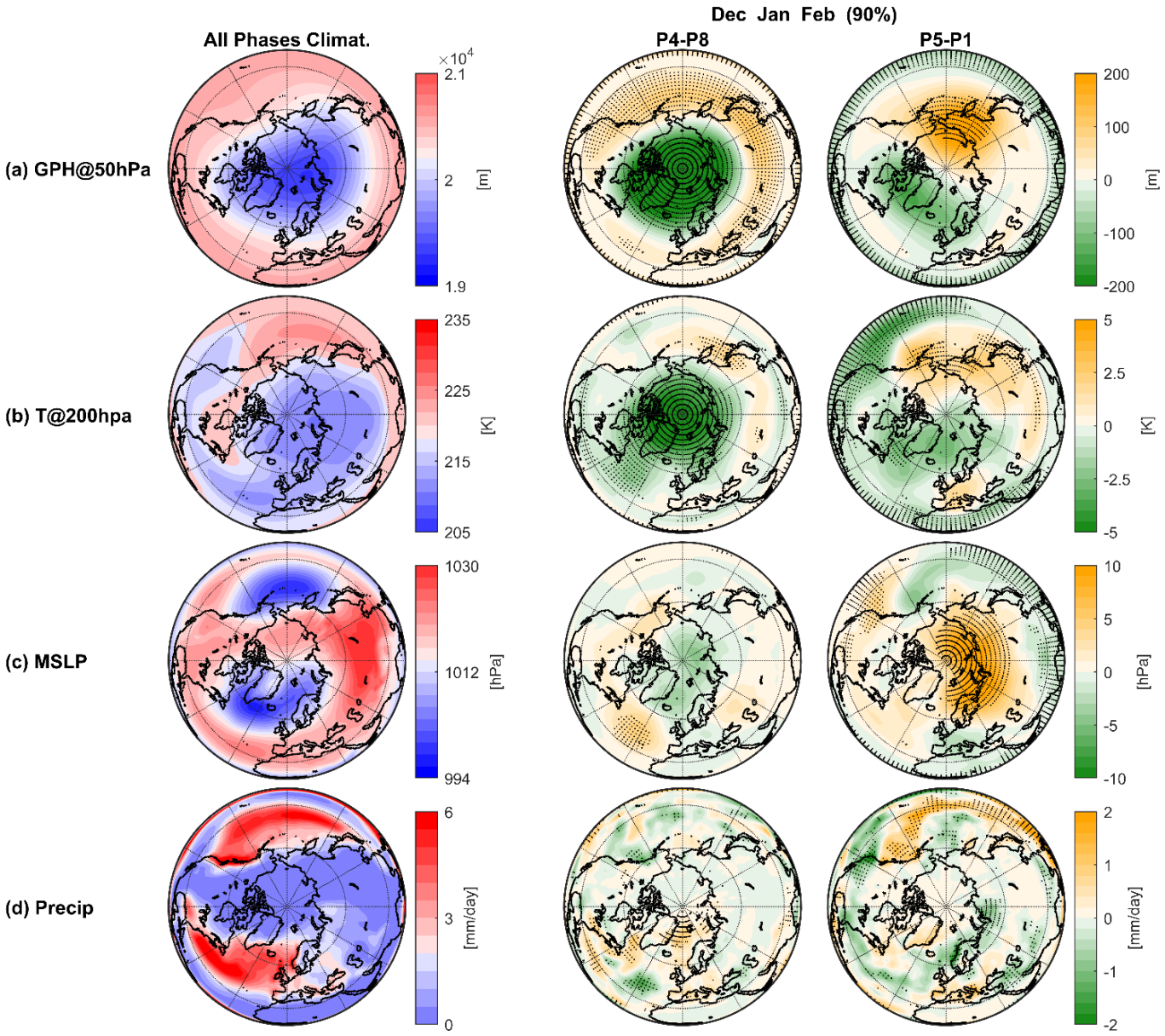

Figure 11. NH orthographic polar projections (10°N–90°N) of a) 50 hPa GPH, b) T at 200 hPa, c) MSLP, and d) precipitation, showing the climatology and anomalies of composite differences between QBO opposite phases during DJF and neutral ENSO. The first, second, and third, columns of each row represent the climatological mean, QBO W – E at 50 hPa (P4 – P8), and QBO W – E at 70 hPa (P5 – P1), respectively. Black dots on the both composite difference plots highlight regions where statistical significance exceeds 90%.

One of the possible mechanisms for the QBO – PNA teleconnection is modulation of the planetary wave train emanating from tropical convection centers along the UTLS pathway (Kumar et al., 2024). They showed that enhanced EP flux convergence in the high latitudes during QBO W at 70hPa. -Increased extratropical stratospheric EP flux convergence favours a low index annual mode for both the SH and NH (Polvani et al., 2010, Fig. 6 of Kumar et al., 2024). Our results

also support the idea that the UTLS pathways involves modulation of the annular~~annular~~ mode, whose primary response is a north -south displacement of the midlatitude jet in a dipole pattern (cf. Plate 4 in Kushner, 2001 and Fig. 4, Kumar et al., 2024).

7. Conclusions

This study presented a brief overview of the GM system ~~as documented in the 42 year climatology,~~ using global monthly mean ERA-5 reanalysis data ~~in the satellite era~~ from 1979 to ~~2022~~2020. We focussed on possible teleconnections between the stratospheric QBO and different monsoon systems at the global scale, in the absence of extreme El Niño and La Niña events. We explored modulation of regional circulations during two different seasons - boreal summer JJA, and austral summer DJF. ~~Composite differences were emphasized for whenever QBO anomaly lies in the lower stratosphere, at 50hPa and 70 hPa. To obtain better insight into QBO pathways for teleconnections with the GM, the seasonal mean canonical form of the QBO anomalies was investigated separately for boreal summer monsoon JJA and austral summer monsoon DJF.~~ Teleconnections were found to vary with ~~the~~ season~~s~~, and to be sensitive to QBO phase. In boreal summer, the subtropical UTLS cold anomaly associated with the MMC during QBO W enhances precipitation associated with the Asian monsoon, spreading eastward over the Northwest Pacific. We also found s~~Previous findings regarding the equatorial QBO routes were confirmed: the tropical subtropical route along the UTLS dominates during the boreal summer JJA. Analysis suggested that the QBO has dynamical teleconnections with different regional monsoons where prominent dynamical circulations prevail, and primarily modulates these circulations, thereby influencing the associated precipitation patterns. S~~ignificant modulations of precipitation patterns ~~were observed across the three main regions of study, the northwest Pacific during JJA, and~~in the North Atlantic and Northeast~~northeast~~ Pacific during DJF.

In the tropics d~~D~~uring JJA, the QBO influences ~~tropical precipitation by~~deep convection and modulates~~ing~~ the WC. QBO W at 50 hPa is accompanied enhanced precipitation near 135°E at the equator (Fig. 5c), which is connected to the region of enhanced precipitation over the subtropical Northwest Pacific (Fig. 5c). When the QBO W anomaly penetrates deeper in the UTLS (70 hPa index P5-P1), precipitation is suppressed near 135°E at the equator (Fig. 5d). This is to be expected in the presence of a large warm anomaly at the tropopause over the Maritime Continent.

~~QBO W at 50 hPa intensifies the Pacific cell of WC (120°E to 225°E), which brings heavier rainfall over the Maritime Continent and less over the Western Pacific. This pattern can be attributed in the modulation of convection, driven by QBO-generated thermal anomalies in the UTLS.~~ A~~In addition, a~~ route along the subtropical UTLS was observed as modulation of circulations over the Northwest Pacific by QBO MMC temperature anomalies, which impacted ~~the associated~~ precipitation in a ~~vast~~ large region extending from China to the Western Pacific. It is confirmed that QBO W at 50 hPa brings ~~lower~~ reduced precipitation over the YHRB region (Zhou at el., 2024). These features were not confined to this region alone, rather, they extended across broader spatial domains, from Japan to the northwestern Pacific Ocean. QBO W at 50 hPa favors a shift in rainfall from the tip of Japan eastward toward a diminished Bonin high. The opposite ~~scenario~~ effects were ~~was~~ observed during QBO E. These patterns can be understood in terms of a regional response to zonally symmetric temperature anomalies

associated with the QBO MMC in the subtropical region that prevailed from northeast Asia to north Pacific region, together with diminution of the Lagrangian overturning circulation between reduced deep convection over the Maritime Continent and a reduced equivalent-barotropic Bonin High.

During DJF, the presence of QBO teleconnection routes along the subtropical UTLS and stratospheric-polar routes were evident through the modulation of precipitation in the extratropics. In the North Atlantic region, QBO W at 50 hPa favors a positive NAO index. This, in turn, enhances the anticyclonic circulation associated with the Azores High, resulting in a more intense NA jet stream and shifts the precipitation maximum westward toward the east coast of North America away from around the Azores High. QBO W at 70 hPa promotes a positive PNA phase, which~~e. As a result, strengthens the anticyclonic circulations over Northeast Pacific, which and~~ intensifies the mid-latitude north~~-~~eastward flow over the Pacific Ocean.~~,~~ ~~which~~ This brings above average precipitation to southern Alaska and below average precipitation on the ~~across the~~ west coast of the United States. The opposite ~~scenarios~~ effects occur for QBO E. On the basis of the current analysis, it is difficult to discern the exact mechanism for these linkages, as most analysis focused on phenomenological descriptions. However, the QBO-NAO linkage may be understood in term of the H-T mechanism associated with the QBO polar route. The NAO and polar vortex have a stronger dynamical ~~tele~~connection ~~with more annular mode structure~~ (Kodera et al., 1999, Kumar et al., 2022). A deeper polar vortex was observed for QBO W than QBO E, affecting the annular mode structure. Another possible mechanism for this linkage may be QBO displacement of the STJs. The QBO-PNA linkage may be due to changes in the pattern of planetary wave radiation along great circle routes from seasonal monsoon system convective centers via the UTLS pathway, with enhanced EP flux convergence in the high latitudes (Kumar et al., 2024). Further detailed investigations are necessary to understand the precise mechanisms operating in the QBO-NAO and QBO-PNA teleconnections.

Data availability statement: All data used in this study are openly accessible for the public.
The ERA-5 data set is available online at https://cds.climate.copernicus.eu/datasets
The OLR data is available online at https://psl.noaa.gov/data/gridded/data.olrcdr.interp.html
The GPCC data is available online at https://psl.noaa.gov/data/gridded/data.gpcc.html
The HadISST data set is available online at https://www.metoffice.gov.uk/hadobs/hadisst/data/download.html

Acknowledgments: The authors would like to thank all members of the ERA5 reanalysis, HadISST, GPCC, and NOAA teams for their efforts in making these datasets available online.

Competing Interests: The authors declare that there are no competing interests.

Research Funding: This paper is based on achievements of the collaborative research project (2025IG-04) of the Disaster Prevention Research Institute of Kyoto University.

Author Contributions: VK and SY jointly worked on the research design and methodology. VK analyzed the all data and wrote the first draft of the paper. MHH, SY, TT, and KI contributed to the conceptualization, review, and edited the draft. MHH also contributed significantly to the discussion section.

References

Adler, R. F., Huffman, G. J., Chang, A., Ferraro, R., Xie, P., Janowiak, J., Rudolf, B., Schneider, U., Curtis, S., Bolvin, D., Gruber, A., Susskind, J., and Arkin, P.: The Version 2 Global Precipitation Climatology Project (GPCP) Monthly Precipitation Analysis (1979–Present), J. Hydrometeor., 4, 1147–1167, 2003.

Adler, R. F., Sapiano, M. R. P., Huffman, G. J., Wang, J.-J., Gu, G., Bolvin, D., Chiu, L., Schneider, U., Becker, A., Nelkin, E., Xie, P., Ferraro, R., and Shin, D.-B.: The Global Precipitation Climatology Project (GPCP) Monthly Analysis (New Version 2.3) and a Review of 2017 Global Precipitation, Atmosphere, 9(4), 138, https://doi.org/10.3390/atmos9040138, 2018.

An Z., Wu G., Li J., Sun Y., Liu Y., Zhou W., Cai Y., Duan A., Li L., Mao J., Cheng H., Shi Z., Tan L., Yan H., Ao H., Chang H., and Feng J.: Global Monsoon Dynamics and Climate Change, Annu. Rev. Earth Planet. Sci., 43, 29-77, https://doi.org/10.1146/annurev-earth-060313-054623, 2015.

Baldwin, M. P., Gray, L. J., Dunkerton, T. J., Hamilton, K., Haynes, P. H., Randel, W. J., and et al.: The quasi-biennial oscillation, Reviews of Geophysics, **39**(2), 179–229, https://doi.org/10.1029/1999RG000073, 2001.

Biasutti, M., Voigt, A., Boos, W. R., Braconnot, P., Hargreaves, J. C., Harrison, S. P., Kang, S. M., Mapes, B. E., Scheff, J., Schumacher, C., Sobel, A. H., and Xie, S.-P.: Global energetics and local physics as drivers of past, present and future monsoons, Nature Geoscience, 11(6), 392–400, https://doi.org/10.1038/s41561-018-0137-1, 2018.

Bordoni, S. and Schneider, T.: Monsoons as eddy-mediated regime transitions of the tropical overturning circulation, *Nature Geoscience*, 1(8), 515–519, https://doi.org/10.1038/ngeo248, 2008.

Brönnimann, S., Malik, A., Stickler, A., Wegmann, M., Raible, C. C., Muthers, S., Anet, J., Rozanov, E., and Schmutz, W.: Multidecadal variations of the effects of the Quasi-Biennial Oscillation on the climate system, Atmos. Chem. Phys., 16, 15529–15543, https://doi.org/10.5194/acp-16-15529-2016, 2016.

Collimore, C. C., Hitchman, M. H., and Martin, D. W.: Is there a quasi-biennial oscillation in tropical deep convection? Geophysical Research Letters, 25(3), 333–336, https://doi.org/10.1029/97GL03722, 1998.

Collimore, C. C., Martin, D. W., Hitchman, M. H., Huesmann, A., and Waliser, D. E.: On The Relationship between the QBO and Tropical Deep Convection, J. Climate, 16, 2552–2568, https://doi.org/10.1175/1520-0442(2003)016<2552:OTRBTQ>2.0.CO;2, 2003.

Chang, C.P., Wang, B. and Lau, N.C.G. Eds.: "The Global Monsoon System: Research and Forecast", WMO/TD, No.1266, pp. 542, https://core.ac.uk/download/pdf/36730348.pdf, 2005.

Chang, C.P., Ding, Y., Lau, N.C., Johnson, R.H., Wang, B., and Yasunari, T. Eds.: "The Global Monsoon System: Research and Forecast (2nd Edition)", World Scientific Series on Asia-Pacific Weather and Climate, 5, pp. 594, 2011.

Chang, C.P., Kuo, H.C., Lau, N.C., Johnson, R.H., Wang, B. and Wheeler, M.C., Eds.: "The Global Monsoon System: Research and Forecast (3rd Edition)", World Scientific Series on Asia-Pacific Weather and Climate, 9, pp. 385, 2016.

Chang, C.P., Ha, K.J., Johnson, R.H., Kim, D., Lau, G.N.C., and Wang, B. Eds.: "The Multiscale Global Monsoon System", World Scientific Series on Asia-Pacific Weather and Climate, 11, pp. 406, 2020.

Chen, W., Yang, S., and Huang, R. H.: Relationship between stationary planetary wave activity and the East Asian winter monsoon, J. Geophys. Res., 110, D14110, doi:10.1029/2004JD005669, 2005.

Gao, X., Hu, J., Ren, R., and Shen, Y.: Impacts of the stratospheric quasi-biennial oscillation on the tropospheric circulation and climate in the Northeast Asia–North Pacific region in early summer, Atmospheric and Oceanic Science Letters, 16, 3, https://doi.org/10.1016/j.aosl.2022.100319, 2023.

Enomoto, T., Hoskins, B. J., and Matsuda, Y.: The Formation Mechanism of the Bonin High in August, Quarterly Journal of the Royal Meteorological Society 129: 157–158, https://doi.org/10.1256/qj.01.211, 2003.

Garfinkel, C. I. and Hartmann, D. L.: The Influence of the Quasi-Biennial Oscillation on the Troposphere in Winter in a Hierarchy of Models. Part I: Simplified Dry GCMs, J. Atmos. Sci., 68, 1273–1289, https://doi.org/10.1175/2011JAS3665.1, 2011.

Giorgetta, M. A., Bengtsson, L., and Arpe K.: Potential role of the quasi-biennial oscillation in the stratosphere-troposphere exchange as found in water vapor in general circulation model experiments, J. Geophys. Res., 104, 6003–6019, https://doi.org/10.1029/1998jd200112, 1999.

Giorgetta, M. A., Bengtsson L., and Arpe, K.: An investigation of QBO signals in the east Asian and Indian monsoon in GCM experiments, Climate Dyn., 15, 435–450, https://doi.org/10.1007/s003820050292,1999b.

Goswami, B.: Interannual variations of Indian summer monsoon in a GCM: External conditions versus internal feedbacks, J. Clim., 11(4), 501–522, https://doi.org/10.1175/1520-0442(1998)011<0501:IVOISM>2.0.CO;2,1998.

García-Franco, J. L., Gray, L. J., Osprey, S., Chadwick, R., and Martin, Z.: The tropical route of quasi-biennial oscillation (QBO) teleconnections in a climate model, Weather Clim. Dynam., 3, 825–844, https://doi.org/10.5194/wcd-3-825-2022, 2022.

García-Franco, J. L., Gray, L. J., Osprey, S., Jaison, A. M., Chadwick, R., and Lin, J.: Understanding the Mechanisms for Tropical Surface Impacts of the Quasi-Biennial Oscillation (QBO), Journal ofGeophysicalResearch:Atmospheres,128(15), e2023JD038474,https://doi.org/10.1029/2023JD038474,2023.

Gray, W. M., Scheaffer, J. D., and Knaff, J. A.: Influence of the stratospheric QBO on ENSO variability. J. Meteorol. Soc. Jpn., 70 (5), 975–995, https://doi.org/10.2151/jmsj1965.70.5_975, 1992a.

Gray, W. M., Sheaffer, J. D., and Knaff, J. A.: Influence of the stratospheric QBO on ENSO variability, *J. Meteor. Soc. Japan*, **70**, 975–995, https://doi.org/10.2151/jmsj1965.70.5_975,1992b.

Gray, L. J., Anstey, J. A., Kawatani, Y., Lu, H., Osprey, S., and Schenzinger, V.: Surface impacts of the Quasi Biennial Oscillation, Atmos. Chem. Phys., 18, 8227–8247, https://doi.org/10.5194/acp-18-8227-2018, 2018.

Gruber, A. and Krueger, A. F.: The status of NOAA outgoing longwave radiation data set, B. Am. Meteor. Soc., 65, 958–962, 1984.

Geen, R., Bordoni, S., Battisti, D. S., Hui, K.: Monsoons, ITCZs, and the Concept of the Global Monsoon, ReviewsofGeophysics, 58(4), e2020RG000700, https://doi.org/10.1029/2020RG000700, 2020.

Gerber, E.P., Polvani, L.: Stratosphere-troposphere coupling in a relatively simple AGCM: the importance of stratospheric variability, J. Clim., 22, 1920–1933, https://doi.org/10.1175/2008JCLI2548.1, 2009

Harvey, V. L. and Hitchman, M. H.: A climatology of the Aleutian high, J. Atmos. Sci., 53, 2088–2101, 1996

Haynes, P. H., McIntyre, M. E., Shepherd, T. G., Marks, C. J., and Shine, K. P.: On the "downward control" of extratropical diabatic circulations by eddy-induced mean zonal forces, J. Atmos. Sci., 48, 651–678, https://doi.org/10.1175/1520-0469(1991)048<0651:OTCOED>2.0.CO;2., 1991.

Haynes, P., Hitchcock, P., Hitchman, M., Yoden, S., Hendon, H., Kiladis, G., Kodera, K., and Simpson, I.: The influence of the stratosphere on the tropical troposphere, J. Meteorol. Soc. Jpn., 99(4), 803–845, https://doi.org/10.2151/jmsj.2021-040, 2021.

Hersbach, H., Bell, B., Berrisford, P., Hirahara, S., Horányi, A., Muñoz-Sabater, J., Nicolas, J., Peubey, C., Radu, R., Schepers, D., Simmons, A., Soci, C., Abdalla, S., Abellan, X., Balsamo, G., Bechtold, P., Biavati, G., Bidlot, J., Bonavita, M., De Chiara, G., Dahlgren, P., Dee, D., Diamantakis, M., Dragani, R., Flemming, J., Forbes, R., Fuentes, M., Geer, A., Haimberger, L., Healy, S., Hogan, R. J., Hólm, E., Janisková, M., Keeley, S., Laloyaux, P., Lopez, P., Lupu, C., Radnoti, G., de Rosnay, P., Rozum, I., Vamborg, F., Villaume, S., and Thépaut, J.-N.: The ERA5 global reanalysis, Q. J. Roy. Meteorol. Soc., 146, 1999–2049, https://doi.org/10.1002/qj.3803, 2020.

Hitchman, M. H., Yoden, S., Haynes, P. H., Kumar, V., and Tegtmeier, S.: An observational history of the direct influence of the stratospheric quasi-biennial oscillation on the tropical and subtropical upper troposphere and lower stratosphere, J. Meteorol. Soc. Jpn., 99, 239–267, https://doi.org/10.2151/jmsj.2021-012, 2021.

Hitchman, M. H., Huesmann, and A. S.: A seasonal climatology of Rossby wave breaking in the layer 330-2000 K, J. Atmos. Sci., **64**, 1922-1940, https://doi.org/10.1175/JAS3927.1, 2007

Holton, J. R., and Tan, H.-C.: The influence of the equatorial quasi-biennial oscillation on the global circulation at 50 mb, Journal of the Atmospheric Sciences, 37(10), 2200–2208. https://doi.org/10.1175/1520-0469(1980)037<2200: TIOTEQ>2.0.CO;2, 1980.

Holton, J. R., and Tan, H.-C.: The quasi-biennial oscillation in the Northern Hemisphere lower stratosphere, Journal of the Meteorological Society of Japan, 60(1), 140–147. https://doi.org/10.2151/jmsj1965.60.1_140, 1982.

Hu, Z.-Z., Huang, B., KinterIII,J.L., Wu, Z., andKumar, A.: Connection of the stratospheric QBO with global atmospheric general circulation and tropical SST. Part II: interdecadal variations,Climate dynamics 38(1), 25–43, https://doi.org/10.1007/s00382-011-1073-6,2012.

Huang,B.,Hu,Z.-Z.,KinterIII,J.L.,Wu,Z.,andKumar,A.:Connection of stratospheric QBO with global atmospheric general circulation and tropical SST. Part I: methodology and composite life cycle,Climate dynamics, 38(1),1–23,https://doi.org/10.1007/s00382-011-1250-7, 2012.

Hurrell, J. W., Kushnir, Y., Ottersen, G., and Visbeck, M.: An overview of the North Atlantic Oscillation, in: Geophysical Monograph American Geophysical Union, Geophysical Monograph Series, 134, 1–35, https://doi.org/10.1029/134GM01, 2003.

Inoue, M., andTakahashi, M.: Connections between the stratospheric quasi-biennial oscillation and tropospheric circulation over Asia in northern autumn: QBO-troposphere relationship over Asia, J. Geophys. Res.: Atmos., 118(19), 10740–10753, https://doi.org/10.1002/jgrd.50827, 2013.

James, I. N.: Introduction to Circulating Atmospheres, Cambridge University Press, 422, 1994.

Jong, B.-T., M.,Ting, and Seager, R.: El Niño's impact on California precipitation: Seasonality, regionality, and El Niño's intensity, *Environmental Research Letters*, **11**, 054021, https://doi.org/10.1088/1748-9326/11/5/054021, 2016.

Kinnersley, J. S. and Tung, K.: Mechanisms for the Extratropical QBO in Circulation and Ozone, J. Atmos. Sci., 56, 1942–1962, https://doi.org/10.1175/1520-0469(1999)056<1942:MFTEQI>2.0.CO;2, 1999.

Krishnamurti, T.N.: Tropical east west circulations during northern summer, J Atmos Sci 28, 1342–1347, https://doi.org/10.1175/1520-0469(1971)028<1342:TEWCDT>2.0.CO;2, 1971

Krishnamurthy, V. and Goswami, B.N.: Indian Monsoon-ENSO Relationship on Interdecadal Timescale. Journal of Climate, 13, 579-595, https://doi.org/10.1175/1520-0442(2000)013<0579:IMEROI>2.0.CO;2, 2000.

Krishnamurti, T.N., Stefanova, L. and Misra, V.: Chapter 5 Monsoons, in "Tropical Meteorology", Springer Atmospheric Sciences. Springer, 75-119, https://doi.org/10.1007/978-1-4614-7409-8_5, 2013.

Kodera, K., Koide, H., and Yoshimura, H.: Northern Hemisphere winter circulation associated with the North Atlantic oscillation and stratospheric polar-night jet, Geophys. Res. Lett., 26, 443–446, https://doi.org/10.1029/1999GL900016, 1999.

Kumar, V., Dhaka, S., Reddy, K., Gupta, A., Prasad, S. S., Panwar, V., Singh, N., Ho, S.-P., and Takahashi, M.: Impact of quasi-biennial oscillation on the inter-annual variability of the tropopause height and temperature in the tropics: A study using COSMIC/FORMOSAT-3 observations, Atmos. Res., 139, 62–70, https://doi.org/10.1016/j.atmosres.2013.12.014, 2014.

Kumar V., Yoden, S., and Hitchman, M. H.: QBO and ENSO effects on the mean meridional circulation, polar vortex, subtropical westerly jets, and wave patterns during boreal winter, J. Geophys. Res.: Atmos., 127, e2022JD036691, https://doi.org/10.1029/2022JD036691, 2022.

Kumar, V., Hitchman, M.H., Du, W. Dhaka, S.K., and Yoden, S.: Teleconnection of the Quasi-biennial oscillation with boreal winter surface climate in Eurasia and North America, Commun Earth Environ, **5**, 251, https://doi.org/10.1038/s43247-024-01422-7, 2024.

Kushner, P. J., Held, I., and Delworth, T. W.: Southern Hemisphere atmospheric circulation response to global warming, J. Climate, 14, 2238–2249, https://doi.org/10.1175/1520-0442(2001)014<0001:SHACRT>2.0.CO;2, 2001.

Kushner, P.J.: Annular modes of the troposphere and stratosphere, in the stratosphere: dynamics, transport, and chemistry, In: Polvani, L.M., Sobel, A.H., Waugh, D.W. (Eds.), Geophysical Monograph Series, American Geophysical Union, 190, 59–92, 2010

Kushner, P.J., and Polvani, L.: Stratosphere-troposphere coupling in a relatively simple AGCM: the role of eddies, J. Clim., 17, 629–639, https://doi.org/10.1175/1520-0442(2004)017<0629:SCIARS>2.0.CO;2, 2004

Lee, J.-H., Kang, M.-J., and Chun, H.-Y.: Differences in the Tropical Convective Activities at the Opposite Phases of the Quasi-Biennial Oscillation. Asia-Pacific J. Atmos Sci., 55, 317–336, 55(3), https://doi.org/10.1007/s13143-018-0096-x, 2019.

Liess, S. and Geller, M. A.: On the relationship between QBO and distribution of tropical deep convection, J. Geophys. Res., 117, 2011JD016317, https://doi.org/10.1029/2011JD016317, 2012.

Ma, T., Chen, W., Huangfu, J., Song, L., and Cai, Q.: The observed influence of the Quasi-Biennial Oscillation in the lower equatorial stratosphere on the East Asian winter monsoon during early boreal winter, International Journal of Climatology, https://doi.org/10.1002/joc.7192, 2021.

Meehl, G. A.: The annual cycle and interannual variability in the tropical Pacific and Indian Ocean regions, Mon. Weather Rev., 115, 27–50, https://doi.org/10.1175/1520-0493(1987)115<0027:TACAIV>2.0.CO;2,1987.

Mooley, D.A., and Parthasarathy, B.: Fluctuations in All-India summer monsoon rainfall during 1871–1978, Climatic Change, 6, 287–301, https://doi.org/10.1007/BF00142477, 1984.

Muhsin, M., Sunilkumar, S. V., Venkat Ratnam, M., Parameswaran, K., Krishna Murthy, B., and Emmanuel, M.: Effect of convection on the thermal structure of the troposphere and lower stratosphere including the tropical tropopause layer in the South Asian monsoon region, J. Atmospheric Sol.-Terr. Phys., 169, 52–65, https://doi.org/10.1016/j.jastp.2018.01.016, 2018.

Naito, Y.: Planetary wave diagnostics on the QBO effects on the deceleration of the polar-night jet in the Southern Hemisphere, J. Meteor. Soc. Japan, 80-4B, 985–995, https://doi.org/10.2151/jmsj.80.985, 2002.

Nie, J. and Sobel, A. H.: Responses of Tropical Deep Convection to the QBO: Cloud-Resolving Simulations,Journal of the Atmospheric Sciences, 72(9), 3625–3638,https://doi.org/10.1175/JAS-D-15-0035.1, 2015.

Pena-Ortiz, C., Ribera, P., Garc ˜ ´ıa-Herrera, R., Giorgetta, M. A., and Garc´ıa, R. R.: Forcing mechanism of the seasonally asymmetric quasi-biennial oscillation secondary circulation in ERA-40 and MAECHAM5, J. Geophys. Res., 113, D16103, doi:10.1029/2007JD009288, 2008.

Polvani, L. M., Sobel, A. H., and Waugh D. W.: The Stratosphere: Dynamics, Transport, and Chemistry, Geophys. Monogr. Ser., 190, AGU, https://doi.org/10.1029/GM190, 2010.

Postel, G. A., and Hitchman, M. H.: Climatology of Rossby wave breaking along the subtropical tropopause, J. Atmos. Sci., 56, 359-373, https://doi.org/10.1175/1520-0469(1999)056<0359:ACORWB>2.0.CO;2, 1999.

Postel, G. A., and Hitchman, M. H.: Observational diagnosis of a Rossby wave breaking event along the subtropical tropopause, Mon. Wea. Rev., 129, 2555-2569, https://doi.org/10.1175/1520-0493(2001)129<2555:ACSORW>2.0.CO;2, 2001.

Randel, W. J., Wu, F., Swinbank, R., Nash, J., and O'Neill, A.: Global QBO circulation derived from UKMO stratospheric analyses, J. Atmos. Sci., 56, 457–474, https://doi.org/10.1175/1520-0469(1999)056<0457:GQCDFU>2.0.CO;2, 1999

Rayner, N. A., Parker, D. E., Horton, E. B., Folland, C. K., Alexander, L., Rowell, D. P., Kent, E. C., and Kaplan, A.: Global analyses of sea surface temperature, sea ice, and night marine air temperature since the late nineteenth century, Journal of Geophysical Research, 108(D14), 4407, https://doi.org/10.1029/2002JD002670, 2003

Reid, G. C. and Gage, K. S.: Interannual variations in the height of the tropical tropopause, J. Geophys. Res.-Atmos., 90, 5629–5635, https://doi.org/10.1029/JD090iD03p05629, 1985

Rodrigo, M., García-Serrano, J., and Bladé, I.: Quasi-biennial oscillation influence on tropical convection and El Niño variability,Geophysical Research Letters, 52(10), e2024GL112854, https://doi.org/10.1029/2024GL112854, 2025.

Schwendike, J., Govekar, P., Reeder, M. J., Wardle, R., Berry, G. J., and Jakob, C.: Local partitioning of the overturning circulation in the tropics and the connection to the Hadley and Walker circulations, J. Geophys. Res.-Atmos., 119, 1322–1339, 2014.

Seo, J., Choi, W., Youn, D., Park, D.-S. R., and Kim, J. Y.: Relationship between the stratospheric quasi-biennial oscillation and the spring rainfall in the western North Pacific, Geophys. Res. Lett., 40, 5949–5953, https://doi.org/10.1002/2013GL058266, 2013.

Shen, S., and Lau, K. M.: Biennial oscillation associated with the East Asian summer monsoon and tropical sea surface temperatures, J. Meteor. Soc. Japan,73,105–124, https://doi.org/10.2151/jmsj1965.73.1_105, 1995.

Tegtmeier, S., Anstey, J., Davis, S., Ivanciu, I., Jia, Y., McPhee, D., and Pilch Kedzierski, R.: Zonal Asymmetry of the QBO Temperature Signal in the Tropical Tropopause Region, Geophys. Res. Lett., 47, e2020GL089533, https://doi.org/10.1029/2020GL089533, 2020.

Thompson, D. W. J. and Wallace, J. M.: Annular modes in the extratropical circulation. Part I: Month-to-month variability, J. Climate, 13, 1000–1016, https://doi.org/10.1175/1520-0442(2000)013<1000:AMITEC>2.0.CO;2, 2000.

Thompson, D. W., and Wallace, J. M.: Regional climate impacts of the Northern Hemisphere annular mode, Science, 293, 85–89, doi:10.1126/science.1058958, 2001.

Wallace, J. M., Panetta, R. L., and Estberg, J.: Representation of the equatorial stratospheric Quasi-Biennial Oscillation in EOF phase space, *J. of the Atm. Scie.*, 50(12), 1751–1762, https://doi.org/10.1175/15200469(1993)050<1751 :ROTESQ >2.0.CO;2, 1993.

Wang, B. and Ding, Q.: Global monsoon: Dominant mode of annual variation in the tropics, Dyn. of Atmos. and Oceans, 44, 165-183, https://doi.org/10.1016/j.dynatmoce.2007.05.002, 2008.

Wang, P.X., Wang, B., Cheng, H., Fasullo, J., Guo, Z.T., Kiefer, T. and Liu, Z.Y.: The global monsoon across time scales: Mechanisms and outstanding issues, Earth-Sci. Rev., 174, 84-121, https://doi.org/10.1016/j.earscirev.2017.07.006, 2017.

Yasunari, T.: Impact of Indian monsoon on the coupled atmosphere/ocean systems in the tropical Pacific, *Meteor. Atmos. Phys.*, 44**,** 29–41. https://doi.org/10.1007/BF01026809, 1990.

Wang, Y.L., Jin, F. F., Wu, C.R., and Qiu, B:Northwestern Pacific Oceanic circulation shaped by ENSO, *Sci. Rep*, 14, 11684,https://doi.org/10.1038/s41598-024-62361-z, 2024.

Wendler, G. Gordon, T., and Stuefer, M: On the Precipitation and Precipitation Change in Alaska, Atmosphere, 2017, 8, 253,https://doi.org/10.3390/atmos8120253, 2017.

Yoden, S., Kumar, V., Dhaka, S.K. and Hitchman, M.H.: Global monsoon systems and their modulation by the equatorial Quasi-Biennial Oscillation. MAUSAM, 74-2 (SPECIAL ISSUE IWM-7 2023), 239-252, https://doi.org/10.54302/mausam.v74i2.5948, 2023.

Yu, S. Y., Fan, L., Zhang, Y., Zheng, X. T. and Li, Z.: Re-examining the Indian summer monsoon rainfall–ENSO relationship from its recovery in the 21st century: Role of the Indian Ocean SST anomaly associated with types of ENSO evolution, Geo. Res. Lett., 48, e2021GL092873, https://doi.org/10.1029/2021GL092873, 2021.

Zhou, F., Wu, Y., Han, T., and Yin, Z.: Stratospheric quasi-biennial oscillation modulates the impact of boreal summer intraseasonal oscillation on rainfall extremes in the Yangtze–Huaihe River Basin, Geophysical Res. Lett., 51, e2024GL110922, https://doi.org/10.1029/2024GL110922s, 2024.

Zuo, J., Xie, F., Yang, L., Sun, C., Wang, L., and Zhang R.: Modulation by the QBO of the relationship between the NAO and Northeast China temperature in late winter, J. Clim., 35, 4395–411, https://doi.org/10.1175/JCLI-D-22-0353.1,2022.